



Research Repository UCD

Title	Mitigating the structural vibrations of wind turbines using tuned liquid column damper considering soil-structure interaction
Authors(s)	Buckley, Tadhg, Watson, Phoebe, Cahill, Paul, Jaksic, Vesna, Pakrashi, Vikram
Publication date	2018-05-01
Publication information	Buckley, Tadhg, Phoebe Watson, Paul Cahill, Vesna Jaksic, and Vikram Pakrashi. "Mitigating the Structural Vibrations of Wind Turbines Using Tuned Liquid Column Damper Considering Soil-Structure Interaction." Elsevier, May 1, 2018. https://doi.org/10.1016/j.renene.2017.12.090 .
Publisher	Elsevier
Item record/more information	http://hdl.handle.net/10197/10350
Publisher's statement	This is the author's version of a work that was accepted for publication in Renewable Energy. Changes resulting from the publishing process, such as peer review, editing, corrections, structural formatting, and other quality control mechanisms may not be reflected in this document. Changes may have been made to this work since it was submitted for publication. A definitive version was subsequently published in Renewable Energy (120, (2018)) https://doi.org/10.1016/j.renene.2017.12.090
Publisher's version (DOI)	10.1016/j.renene.2017.12.090

Downloaded 2025-12-04 23:04:11

The UCD community has made this article openly available. Please share how this access benefits you. Your story matters! (@ucd_oa)



© Some rights reserved. For more information

Mitigating the Structural Vibrations of Wind Turbines using Tuned Liquid Column Damper Considering Soil-Structure Interaction

by

Tadhg Buckley¹, Phoebe Watson², Paul Cahill³, Vesna Jaksic⁴ and Vikram Pakrashi^{*5}

^{1,5} Dynamical Systems and Risk Laboratory, School of Mechanical and Materials Engineering,
University College Dublin, Ireland and Marine and Renewable Energy Ireland (MaREI) Centre,
University College Dublin, Ireland

² Arup, Dublin, Ireland

³ Marine and Renewable Energy Ireland (MaREI) Centre, University College Cork, Ireland

⁴ Civil, Structural and Environmental Engineering, Cork Institute of Technology, Ireland

E-mail: ¹p.j.watson@umail.ucc.ie, ²tadhgbuckley@umail.ucc.ie, ³p.a.cahill@umail.ucc.ie,

⁴V.Jaksic@ucc.ie, ⁵vikram.pakrashi@ucd.ie

* Corresponding Author

19
20
21
22
23
24
25
26
27
28
29
30
31
32
33
34
35
36
37
38

Abstract

This paper considers the potential of using a Tuned Liquid Column Damper (TLCD) to reduce structural vibrations of a wind turbine tower. The effect of TLCD on wind turbine towers, including the soil-structure interactions for a monopile foundation was modelled theoretically and scaled laboratory experiments were carried out to validate these results. The tower of the turbine is represented as an Euler beam with a set of springs at the boundary to simulate the soil-structure interaction. TLCD design was carried out using such a model and the reduction in tower vibrations due to the deployment of TLCD was then examined for various loading conditions in the frequency and the time domain. The efficiency of TLCDs for reducing structural vibrations was investigated for tuned and detuned conditions. The response of a small-scale model was simulated along with that of a full-scale turbine and parametric studies around the variations of inputs related to uncertainties were performed. Experiments were carried out on a scaled model turbine to examine the effectiveness of the TLCD. The practicalities of installing a TLCD in a full-scale turbine were examined.

Keywords: Wind Turbine, Soil-Structure Interaction, Tuned Liquid Column Damper, Experiments, Vibrations

39 Key Nomenclature

40 Symbols

E	Young's modulus of the turbine tower
I	Second moment of area of the cross-section of the turbine tower
x	Spatial coordinate along the length of the turbine tower, measured from the base
t	Time measured from when the excitation was applied,
$y(x, t)$	Dynamic deflection of the turbine tower
m	Mass per unit length of the turbine tower
$f(x, t)$	Time dependant distributed load applied to the turbine tower
P	Constant axial force applied to the turbine tower
r	Radius of gyration of the turbine tower
J	Moment of Inertia of the nacelle
L	Length of turbine tower
M_s	Mass of the primary system
$W(\xi)$	Lateral displacement in terms of ξ
Ω	Non-dimensional frequency parameter
v	Non-dimensional axial force
η_r	Non-dimensional rotational foundation stiffness
η_l	Non-dimensional lateral foundation stiffness
α_t	Mass ratio of nacelle to turbine tower
β_t	Non-dimensional rotary inertia
μ_t	Non-dimensional radius of gyration
c_0	Natural frequency scaling parameter
ω_n	First natural frequency
C_s	Damping of the primary system

K_s	Response of the primary system
$x(t)$	Displacement of the primary system with respect to time
$\dot{x}(t)$	Velocity of the primary system with respect to time
$\ddot{x}(t)$	Acceleration of the primary system with respect to time
$f(t)$	Time dependant load applied to the primary system
X_s	Dynamic displacement response of the primary structure with respect to time
x_f	Dynamic displacement response of the liquid damper with respect to time
g	Acceleration due to gravity
Δ	Represent application of base excitation when equal to one and is zero otherwise.
m_d	Mass of liquid in the TLCD
k_f	Stiffness of the liquid column
c_{eq}	Linearized damping coefficient replacing the nonlinear damping of the TLCD
A	Cross sectional area of TLCD
l	Total length of column of water
$\bar{\xi}$	Head loss coefficient
α	Length ratio of the TLCD
μ_s	Mass ratio of TLCD to Primary System
ζ_s	Damping ratio of TLCD to primary system
γ_s	Tuning ratio of TLCD to primary system
ζ_{opt}	Optimum damping ratio
γ_{opt}	Optimum tuning ratio
$F(\omega)$	Forcing function in frequency domain
$H(i\omega)$	Transfer function describing the conversion from time to frequency domain
ω_d	Natural frequency of the TLCD

ω_f	Natural frequency of oscillating liquid
ζ_d	Damping ratio of the TLCD
ω	Frequency of the load applied to the structure
k	Equivalent modulus of the subgrade reaction
L_c	Critical pile length
G	Shear modulus of the soil
E_p	Youngs modulus of monopile
I_p	Moment of inertia of the pile
k_l	Lateral stiffness of the spring representing the soil-structure interaction
k_r	Rotational stiffness of the spring representing the soil-structure interaction
k	Equivalent modulus of the subgrade reaction
d_{50}	Average grain size
t	Thickness of the tower
M_n	Mass of the nacelle
ρ	Density of fluid in TLCD
ρ_T	Density of the material used for the turbine tower
D	Diameter of turbine tower
t	Average thickness of turbine tower
$H(i\omega)_{Max}$	Maximum response of transfer function

41 Key Abbreviations

TLCD	Tuned Liquid Column Damper
TMD	Tuned Mass Damper

43

44 **1 INTRODUCTION**

45 Wind turbines have evolved to be taller and more slender over time to harness more energy and
46 consequently the dynamic responses of wind turbines superstructure and related control of
47 unwanted dynamic responses have become very important [1, 2]. Control of unwanted structural
48 vibrations can lead to a longer life of wind turbines by decreasing stress and related fatigue [3].
49 A reduction in tower vibration is also related to the reduction of gearbox faults [4]. Additionally,
50 control of tower vibrations can lead to a reduction of loads on the foundation, which are often a
51 significant part of the project cost [5]. Overall, vibration control of wind turbine towers can lead
52 to better built wind turbines with longer and healthy life span.

53 Most literature in wind turbine vibration control concentrate on passive [6-8] or semi-active [9-
54 11] control systems and algorithms. Design choice of materials has also been studied for
55 improved fragility of wind turbine towers [12]. Of these systems, the passive control systems,
56 typically Tuned Mass Dampers (TMDs) and Tuned Liquid Column Dampers (TLCDs) are
57 particularly popular as they do not require external power to operate. Practical implementation
58 constraints like weight, geometry, connection with the primary structure, and the lifespan of the
59 control system are present for these vibration control methods, but the fundamentals behind
60 passive control through TMD and TLCD are mainly related to the tuning of the natural
61 frequency of the spring mass system (for TMD) or the oscillating water column (for TLCD) to
62 the natural frequency of the primary structure. As long as there is sufficient mass or in the case
63 of TLCD, some additional friction loss due to oscillation of fluids against the tubular structure
64 where the liquid is retained, control is achieved. Optimisation of control can then be carried out

by carefully choosing the design parameters [13]. Recently, a number of studies on single and multiple TLCDs applied to onshore wind turbine towers and floating wind turbine platforms [14, 15] have indicated that TLCDs may be a reasonable way to reduce wind turbine tower vibrations.

Despite the advantages of TLCDs, a drawback remains regarding the fact that the success of TLCDs strongly depends on the tuning of the oscillating liquid column with that of the primary structure to which it is attached. The natural frequency of a wind turbine tower can vary for the same manufactured tower, based on what soil it is embedded into and how it is embedded. Based on such situations, the boundary conditions of the wind turbine towers vary and so do their natural frequencies as function of soil-structure interaction [16, 17]. In fact, such variation is not necessarily a change from one site to another, but can take place over the lifespan of turbines at a single site [18]. Consequently, designing a TLCD for a factory manufactured wind turbine tower may not be sufficient since detuning can take place due to soil-structure interaction. Under such circumstances, it is important to assess the performance of TLCDs in the presence of soil-structure interaction. This paper investigates the performance of TLCD for the vibration control of wind turbine towers considering soil-structure interaction. A well-known model is considered, based on first principles and a detailed numerical study is carried out for this purpose in the time and the frequency domains. Effects of detuning are investigated. A non-dimensional theoretical model is created for the system investigated and predicted dynamic responses are compared against a laboratory based small-scale experimental model to validate the numerical investigations. The importance of considering soil-structure interactions for vibration control of wind turbine towers using TLCD is emphasized through this study and aspects of practical

implementation are also discussed. A number of assumptions are related to this study. These include the modelling of the tower as an Euler-Bernoulli cantilever monopile beam with the nacelle as a tip mass on the cantilever, the choice of soil properties in the form of a spring, consideration of the boundary conditions as a combination of a linear and a rotational spring representing the interaction between the structure and soil and dependent on shear modulus and bending rigidity of the pile, the achievement of scaling is through non-dimensionalisation of governing equations and limiting the diameter of the pile to average grain size ratio. Details around these assumptions are presented in each sub-section of the paper.

It is noted that despite several studies around tuned liquid column dampers and soil-structure interaction, there is a gap in terms of integrating the two aspects and investigating this interrelation in detail. This work attempts to address this gap in a timely manner and presents a comprehensive study following a consistent formulation for both passive damping and soil-structure interaction. The paper also provides clear guidance of scaling and development of experiments corresponding to such scaling for this purpose. The comprehensive investigation presented is expected to provide practical engineering guidance for the integrated design of such dampers and aid in making the sector more competitive.

2 THEORETICAL MODELLING OF A WIND TURBINE WITH A TLCD CONSIDERING SOIL-STRUCTURE INTERACTION

The theoretical model presented here integrated two established and importance models in the field of soil-structure interaction of a wind turbine and passive control through TLCD respectively to create a unified numerical framework which can allow consistent non-dimensionalization of both aspects and allow for a comprehensive numerical analysis. The models are referenced and are summarised in two sub-sections for the purpose of completeness, clarity and context of the simulations presented in the rest of the work. The models and the non-dimensionalization presented in the next sections also for the basis of designing experimentation for this paper.

2.1 Formulation of the soil-structure interaction model of wind turbine towers

An idealised model of a wind turbine tower is considered in Figure 1 based on [19], where the tower is modelled as an Euler-Bernoulli beam, while the nacelle is represented as a tip mass at the free end of the beam. The soil-structure interaction is modeled as boundary conditions specified by spring whose characteristics are related to soil properties. It is assumed that properties such as Young's modulus, moment of inertia, axial loading and mass per metre of tower are constant along the length of the tower, the tower is in a state of equilibrium and a harmonic solution for deflection with respect to time and distance exists.

FIGURE 1 HERE

The equation of motion of an Euler-Bernoulli beam can then be used to represent the dynamics of the turbine tower as

$$\frac{\partial^2}{\partial x^2} \left(EI(x) \frac{\partial^2 y(x,t)}{\partial x^2} \right) + \frac{\partial}{\partial x} \left(P \frac{\partial y(x,t)}{\partial x} \right) - \frac{\partial}{\partial x} \left(m(x) r^2 \frac{\partial \ddot{y}(x,t)}{\partial x} \right) + m(x) \ddot{y}(x,t) = f(x,t) \quad (1)$$

127 where $y(x, t)$ is the dynamic deflection of the turbine tower as shown in Figure 1, $f(x, t)$ is a
 128 time-dependant distributed load applied to the turbine tower, x is the spatial coordinate along the
 129 length of the turbine tower, measured from the base, t is the time measured from when the
 130 excitation was applied, E is the Young's modulus of the turbine tower, I is the second moment
 131 of area of the cross-section turbine tower about the neutral axis of bending, P is a constant axial
 132 force applied to the turbine tower, m is the mass per unit length of the turbine tower obtained by
 133 dividing density with cross-sectional area, r is the radius of gyration of the turbine tower and an
 134 overdot is a derivative with respect to time.

135 Assuming all properties are constant along the length of the tower, this equation can be
 136 simplified to

$$137 \quad EI \frac{\partial^4 y(x, t)}{\partial x^4} + P \frac{\partial^2 y(x, t)}{\partial x^2} - mr^2 \frac{\partial^2 \ddot{y}(x, t)}{\partial x^2} + m\ddot{y}(x, t) = f(x, t) \quad (2)$$

138 For equilibrium, the total sum of the bending moments and the total sum of the shear forces must
 139 equal to zeros at the end. Considering boundary conditions at $x=0$, there is some lateral and
 140 rotational freedom but no vertical movement is allowed. Considering the bending and shear
 141 equilibrium at the end of the tower respectively, we obtain

$$142 \quad EI \frac{\partial^2 y(0, t)}{\partial x^2} - k_r \frac{\partial y(0, t)}{\partial x} = 0 \quad (3)$$

$$143 \quad EI \frac{\partial^3 y(0, t)}{\partial x^3} + P \frac{\partial y(0, t)}{\partial x} + k_l w(x, t) - mr^2 \frac{\partial^2 \ddot{y}(0, t)}{\partial x^2} = 0 \quad (4)$$

144 where k_r and k_l are the rotational and lateral stiffness of the springs, respectively, which
 145 represent the soil-structure interaction.

146 The other boundary of the beam at $x = L$ allows rotational and lateral freedom, assuming
 147 sufficient axial stiffness such that no vertical deflection takes place. Under such circumstances,
 148 the consideration moment and shear equilibrium respectively, gives

$$149 \quad EI \frac{\partial^2 y(L, t)}{\partial x^2} + J \frac{\partial \dot{y}(L, t)}{\partial x} = 0 \quad (5)$$

150 and

$$151 \quad EI \frac{\partial^3 y(L, t)}{\partial x^3} + P \frac{\partial y(L, t)}{\partial x} - M \ddot{y}(L, t) - mr^2 \frac{\partial^2 \ddot{y}(L, t)}{\partial x^2} = 0 \quad (6)$$

152 Assuming a harmonic solution $y(x, t) = W(\xi) \exp\{i\omega t\}$, where $\xi = x/L$, and substituting into
 153 the previous equations gives

$$154 \quad \frac{EI}{L^4} \frac{\partial^4 W(\xi)}{\partial \xi^4} + \frac{P}{L^2} \frac{\partial^2 W(\xi)}{\partial \xi^2} - m\omega^2 W(\xi) + \frac{mr^2\omega^2}{L^2} \frac{\partial^2 W(\xi)}{\partial \xi^2} = f(\xi) \quad (7)$$

$$155 \quad \frac{EI}{L^2} W''(0) - \frac{k_r}{L} W'(0) = 0 \quad (8)$$

$$156 \quad \frac{EI}{L^3} W'''(0) + \frac{P}{L} W'(0) + k_l W(0) + \frac{mr^2\omega^2}{L} W'(0) = 0 \quad (9)$$

$$157 \quad \frac{EI}{L^2} W''(1) + \frac{\omega^2 J}{L} W'(1) = 0 \quad (10)$$

158 and

$$159 \quad \frac{EI}{L^3} W'''(1) + \frac{P}{L} W'(1) + \omega^2 MW(1) + \frac{mr^2\omega^2}{L} W'(1) = 0 \quad (11)$$

160

161 Rearranging in terms of non-dimensional parameters, these equations can be written as

$$162 \quad \frac{\partial^4 W(\xi)}{\partial \xi^4} + \tilde{v} \frac{\partial^2 W(\xi)}{\partial \xi^2} - \Omega^2 W(\xi) = F(\xi) \frac{L^2}{EI} \quad (12)$$

$$163 \quad W''(0) - \eta_r W'(0) = 0 \quad (13)$$

$$164 \quad W'''(0) + \tilde{v} W'(0) + \eta_l W(0) = 0 \quad (14)$$

$$165 \quad W''(1) - \beta \Omega^2 W'(1) = 0 \quad (15)$$

166 and

$$167 \quad W'''(1) + \tilde{v} W'(1) + \alpha \Omega^2 W(1) = 0 \quad (16)$$

168 Where

$$169 \quad \tilde{v} = v + \mu_t^2 \Omega^2 \quad (17)$$

170 The definitions of the non-dimensional parameters defined in this derivation is shown in Table 1.

171 Table 1. Non-dimensional parameters in wind turbine tower dynamics formulation with soil-
172 structure interaction.

Non-dimensional axial force	$v = \frac{PL^2}{EI}$
Non-dimensional rotational foundation stiffness	$\eta_r = \frac{k_r L}{EI}$
Non-dimensional lateral foundation stiffness	$\eta_l = \frac{k_l L^3}{EI}$
Non-dimensional frequency parameter	$\Omega = \sqrt{\omega^2 \frac{mL^4}{EI}}$
Mass ratio of nacelle to turbine tower	$\alpha_t = \frac{M}{mL}$

Non-dimensional rotary inertia	$\beta_t = \frac{J}{mL^3}$
Non-dimensional radius of gyration	$\mu_t = \frac{r}{L}$

173

174 The natural frequency can then be described as $\omega_j = \Omega_j c_0$ where the natural frequency scaling

175 parameter is defined as $c_0 = \sqrt{\frac{EI}{mL^4}}$

176 Assuming a solution for the lateral displacement y with respect to x of the form $W(\xi) =$

177 $\exp\{\lambda\xi\}$ allows for the separation of the time and distance variables. Substituting into the Euler

178 equation governing the behaviour of the tower gives

$$179 \quad \lambda^4 + \tilde{\nu}\lambda^2 - \Omega^2 = 0 \quad (18)$$

180 A solution to this equation is

$$181 \quad \lambda = \pm i\lambda_1, \pm\lambda_2 \quad (19)$$

182 where

$$183 \quad \lambda_1 = \left(\sqrt{\left(\frac{\tilde{\nu}}{2}\right)^2 + \Omega^2} + \frac{\tilde{\nu}}{2} \right)^{1/2} \quad (20)$$

$$184 \quad \lambda_2 = \left(\sqrt{\left(\frac{\tilde{\nu}}{2}\right)^2 + \Omega^2} - \frac{\tilde{\nu}}{2} \right)^{1/2} \quad (21)$$

185 Using eigenvectors to re-write the solution for $W(\xi)$ as

$$186 \quad W(\xi) = a_1 \sin(\lambda_1 \xi) + a_2 \cos(\lambda_1 \xi) + a_3 \sinh(\lambda_2 \xi) + a_4 \cosh(\lambda_2 \xi) \quad (22)$$

187 Rearranging this in matrix form gives

$$188 \quad W(\xi) = \mathbf{s}^T(\xi)\mathbf{a} \quad (23)$$

189 where $\mathbf{s}(\xi) = \{\sin(\lambda_1\xi), \cos(\lambda_1\xi), \sinh(\lambda_2\xi), \cosh(\lambda_2\xi)\}^T$ and $\mathbf{a} = \{a_1, a_2, a_3, a_4\}^T$

190 Applying this solution to the boundary condition equations obtained previously gives the
191 following equations

$$192 \quad \frac{d^2}{d\xi^2}(\mathbf{s}^T(0)\mathbf{a}) - \eta_r \frac{d}{d\xi}(\mathbf{s}^T(0)\mathbf{a}) = 0 \quad (24)$$

$$193 \quad \frac{d^3}{d\xi^3}(\mathbf{s}^T(0)\mathbf{a}) + \tilde{v} \frac{d}{d\xi}(\mathbf{s}^T(0)\mathbf{a}) + \eta_l \mathbf{s}^T(0)\mathbf{a} = 0 \quad (25)$$

$$194 \quad \frac{d^2}{d\xi^2}(\mathbf{s}^T(1)\mathbf{a}) - \beta\Omega^2 \frac{d}{d\xi}(\mathbf{s}^T(1)\mathbf{a}) = 0 \quad (26)$$

$$195 \quad \frac{d^3}{d\xi^3}(\mathbf{s}^T(1)\mathbf{a}) + \tilde{v} \frac{d}{d\xi}(\mathbf{s}^T(1)\mathbf{a}) + \alpha\Omega^2 \mathbf{s}^T(1)\mathbf{a} = 0 \quad (27)$$

196 which becomes

$$197 \quad -\eta_r \lambda_1 a_1 - \lambda_1^2 a_2 - \eta_r \lambda_2 a_3 + \lambda_2^2 a_4 = 0 \quad (28)$$

$$198 \quad (-\lambda_1^3 + \tilde{v}\lambda_1)a_1 + \eta_l a_2 + (\lambda_2^3 + \tilde{v}\lambda_1)a_3 + \eta_l a_4 = 0 \quad (29)$$

$$199 \quad (-\lambda_1^2 \sin(\lambda_1) - \beta\Omega^2 \lambda_1 \cos(\lambda_1))a_1 + (-\lambda_1^2 \cos(\lambda_1) + \beta\Omega^2 \lambda_1 \sin(\lambda_1))a_2 + (\lambda_2^2 \sinh(\lambda_2) - \\ 200 \quad \beta\Omega^2 \lambda_2 \cosh(\lambda_2))a_3 + (\lambda_2^2 \cosh(\lambda_2) - \beta\Omega^2 \lambda_2 \sinh(\lambda_2))a_4 = 0 \quad (30)$$

determining the vibration absorber parameters for an un-damped system has proved successful in developing the equations of motion for a TLCD [13]. Using Den Hartog's [21] methods, analytical formulas for determining the equations of motion for a uniform cross-sectional area TLCD have been long derived by Sakai and Takaeda [22]. When the wind turbine is subjected to a dynamic load, movement will result in the liquid contained within the attached TLCD. From D'Alembert's principle, the inertia force of water is

$$I_M = -[\rho A l \ddot{x}_f(t) + \rho A b \ddot{X}_s(t)] \quad (33)$$

Where ρ is the density of the fluid, A is the cross sectional area of TLCD, l is the total length of column of water, b is the length of horizontal section of TLCD, x_f is the response of the liquid damper and X_s is the response of the primary system.

The difference of height of water in the vertical columns provides the differential spring force of the TLCD. The restoring force of the water is

$$I_R = \rho A \cdot 2x_f(t) \cdot g \quad (34)$$

$x_f(t)$ being the response of the liquid damper (TLCD) and g the acceleration due to gravity

The damping force is

$$I_D = -\rho A \bar{\xi} \frac{|\dot{x}_f(t)|}{2} \quad (35)$$

with $\bar{\xi}$ as the head loss coefficient, influenced primarily by the diameter of the orifice and by Darcy's friction factor between the liquid and the inner surface of the TLCD walls, the corners of the TLCD etc.

237 From the condition of equilibrium, the equation of motion is given by

$$238 \quad \rho A l \ddot{x}_f(t) + \frac{1}{2} \rho A \bar{\xi} |\dot{x}_f(t)| + 2 \rho A g x_f(t) = -\rho A b \ddot{X}_s(t) \quad (36)$$

239 where the natural frequency of the oscillating liquid is given by $\omega_f = \sqrt{2g/l}$.

240 The equation of motion for a single degree of freedom structure is

$$241 \quad M_s \ddot{x}(t) + C_s \dot{x}(t) + K_s x(t) = f(t) \quad (37)$$

242 Where M_s is the mass of the primary system, C_s is the damping of the primary system, K_s is the
 243 stiffness of the primary system, (t) is the time dependant load applied to the primary system.
 244 $x(t)$ is the displacement, $\dot{x}(t)$ is the velocity and $\ddot{x}(t)$ is the acceleration of the primary system
 245 with respect to time and f .

246 From this, the equation of motion for the wind turbine system is obtained as

$$247 \quad (M_s + \rho A l) \ddot{X}_s(t) + \rho A b \ddot{x}_f(t) + C_s \dot{X}_s(t) + K_s X_s(t) = f(t) \quad (38)$$

248 where $C_s = 2M_s \zeta_s \omega_s$, ζ_s is the damping ratio of the primary system and ω_s is the natural
 249 frequency of the primary system.

250 Coupling the dynamics of the TLCD with that of the wind turbine tower [13] results in

$$251 \quad \begin{bmatrix} M_s + m_d & \alpha m_d \\ \alpha m_d & m_d \end{bmatrix} \begin{bmatrix} \ddot{X}_s \\ \ddot{x}_f \end{bmatrix} + \begin{bmatrix} C_s & 0 \\ 0 & c_{eq} \end{bmatrix} \begin{bmatrix} \dot{X}_s \\ \dot{x}_f \end{bmatrix} + \begin{bmatrix} K_s & 0 \\ 0 & k_f \end{bmatrix} \begin{bmatrix} X_s \\ x_f \end{bmatrix} = \begin{bmatrix} f(t) \\ \frac{\Delta m_d f(t)}{M_s} \end{bmatrix} \quad (39)$$

252 and

$$253 \quad |x_f| \leq \frac{(l-b)}{2} \quad (40)$$

where α is the length ratio of the TLCD and equal to l/b , m_d is the mass of liquid in the TLCD, c_{eq} is a linearized damping coefficient replacing the nonlinear damping $c_{nonlinear}$ of the TLCD equal to $2m_d\zeta_d\omega_d$, ζ_d is the damping ratio of the TLCD, ω_d is the natural frequency of the TLC, k_f is the stiffness of the liquid column equal to $2\rho Ag$, and $f(t)$ is the external excitation. The constraint in equation 40 is to ensure that the liquid does not spill out of the TLCD when sloshing. The time t is measured from when the load is first applied, X_s is the dynamic displacement response of the primary structure with respect to time. This is a relative displacement when $\Delta = 1$ and absolute displacement when $\Delta = 0$. The consideration of $\Delta = 1$ is representative of the application of a base excitation, while $\Delta = 0$ represents a force applied to the structure only. The coupled set of equations can be converted to a state space form and solved using numerical integration methods like the Runge-Kutta approach.

The transfer function for the coupled TLCD-tower equation can be obtained by following Yalla and Kareem [13] as

$$H(i\omega) = \frac{-\Delta\mu\alpha(i\omega)^2 + (i\omega)^2 + 2\zeta_d\omega_d(i\omega) + \omega_d^2}{[(i\omega)^2(1+\mu) + 2\zeta_s\omega_s(i\omega) + \omega_s^2][(i\omega)^2 + 2\zeta_d\omega_d(i\omega) + \omega_d^2] - (i\omega)^4\alpha^2\mu} \quad (41)$$

where α is the tuning ratio of the TLCD, representing the horizontal column width to the full length of the column of water, horizontal and vertical combined. The mass ratio, μ , is the mass of the TLCD over the mass of the structure. The natural frequency of the tower is dependent of soil parameters and so is the transfer function.

2.3 Formulation of soil parameters

The strength of the soil and the bending resistance of the pile are combined to two springs for lateral and rotational resistance, with stiffness k_l and k_r respectively. These values, as derived by Adhikari & Bhattacharya [19], depend on the shear modulus and bending rigidity of the pile and can be expressed by

$$k_l = \frac{k}{\sqrt{2}} \left(\frac{4}{L_c} \right)^{-1} \quad (42)$$

$$k_r = \frac{k}{\sqrt{2}} \left(\frac{4}{L_c} \right)^{-3} \quad (43)$$

where k is the equivalent modulus of the subgrade reaction and L_c is the critical pile length, beyond which the pile behaves as if it were infinitely long.

An approximation for k is given by

$$\frac{k}{G} \approx 10 \left(\frac{E_p}{G} \right)^{-0.14} \quad (44)$$

Where E_p is the Young's modulus of the pile and G is the shear modulus of the soil. The critical length of the pile can then be found using the expression

$$L_c = 4 \left(\frac{E_p I_p}{4k} \right)^{1/4} \quad (45)$$

where I_p is the moment of inertia of the pile.

The soil parameters for numerical studies are taken from data provided by Adhikari & Bhattacharya [19] for the shear modulus of dry sand, saturated sand and clay.

It should also be noted that soil properties change with high cyclic loading, thereby increasing the complexity in understanding the long term behaviour of the turbine and thereby introducing the risk that the natural frequency may change gradually over time [23]. The soil-structure interaction was modelled using the two springs to describe lateral and torsional restraint of the pile in this paper, as has been described earlier. This method, proposed by Adhikari & Bhattacharya [19], has been well documented and validated by experiments, giving reasonably high degree of confidence in the method used.

The importance of scaling cannot be underestimated when drawing conclusions between a small-scale model and full-scale prototype. For this reason, the small-scale theoretical model was designed to be able to scale up to represent some behaviour of a full-scale turbine. The use of non-dimensional parameters in the soil-structure interaction model helped facilitate this. The geometry of the structure for a scaled model was considered at a 1:100 ratio. The soil-structure interaction, as represented by springs representing the lateral and rotational stiffness of the foundations, scale automatically since k_l and k_r are calculated depending on both soil characteristics and bending rigidity of the pile. Care was also taken to ensure that the diameter of the pile to average grain size ratio did not exceed a recommended limit of $D/d_{50} = 88$, where D is the diameter of the pile, in this case equal to that of the turbine tower, and d_{50} is the average grain size [24].

3 NUMERICAL STUDIES ON A WIND TURBINE WITH A TLCD CONSIDERING SOIL-STRUCTURE INTERACTION

3.1 Numerical values for input variables

Initial simulations were done first for a full-scale turbine, with using data from Tempel and Molenaar [20] to test the numerical model against established results as a benchmark. Numerical simulations were then run for the small-scale model turbine to suggest parameters for the experimentation section, based on model testing carried out by [23]. The input data for the simulations are given in Table 2.

Table 2. Input data for numerical simulations on wind turbine tower – TLCD interaction for full-scale and model.

Property	Symbol	Full-scale Turbine	Small-scale Model	Unit
Height	L	81	1.2	m
Diameter	D	3.5	0.03	m
Thickness	T	0.075	0.003	m
Moment of Inertia	I	1.1839	5.123×10^{-8}	m^4
Radius of Gyration	R	1.2112	0.0109	m
Weight of Nacelle	M_s	130000	0.3	kg
Damping Ratio of Tower	ζ_s	0.01	0.01	
Inertia of Nacelle	J	0	0	m^4

The small-scale model was designed in such a way that the results can be scaled up to predict results for a full-scale turbine. The formulas used for the second moment of area (I) and the radius of gyration (r) for the cross-section of the tower with thickness t were $I = \frac{\pi}{64}(D^4 - (D - t)^4)$ and $r = \frac{\sqrt{D^2 - (D - t)^2}}{4}$ respectively. The material properties used for the two models are given in Table 3. The full-scale turbine had a steel tower, while the small-scale model was made of aluminium.

327 Table 3. Material properties of the full-scale and the model wind turbine tower.

Property	Symbol	Steel	Aluminium	Units
Young's Modulus	E	210	69	GPa
Density	ρ	7800	2700	kg/m ³

328

329 The values for k_r and k_l were calculated as described in the previous section and given in Table 4
330 for the full-scale wind turbine tower.

331 Table 4. Boundary conditions of the full-scale wind turbine tower as a function of soil properties.

Property	Bulk Density [kN/m ³]	Shear Modulus [MPa]	k_r [MNm/rad]	k_l [MN/m]
Dry sand	15.73	12.72	152.5	6654.1
Saturated Sand	19.6	8.2	102.6	5830.3
Clay	16.6	2	313.6	3927.4

332

333 The spring constants representing the lateral and rotational stiffness provided by the soil depend
334 on the Young's modulus and moment of inertia of the monopole as well as the soil parameters,
335 so these values were recalculated for the small-scale model as well (Table 5).

336

337 Table 5. Boundary conditions of the small-scale wind turbine tower as a function of soil
338 properties.

Property	Shear Modulus [MPa]	k_r [kNm/rad]	k_l [N/m]
Sand	12.72	1042.2	1554.7
Top Soil	8	701.1	1362.2
Clay	2	214.3	917.6

339

The lateral and rotational stiffness of the springs representing the soil-structure interaction is considerably smaller for the model turbine due to the dependence of this parameter on the moment of inertia of the monopile foundation. The top soil is a typical garden soil with a shear modulus between that of clay and gravel.

The main parameters that govern the effectiveness of a TLCD are the tuning of the natural frequency of the liquid column to that of the host structure and the mass ratio between the TLCD and the host structure. Table 6 presents the baseline values used for the TLCD when considering a full-scale structure and the small-scale experiment. Some of these parameters, such as the damping ratio, mass ratio and length ratio, were varied in the numerical simulations to understand the effect of poor optimisation of the TLCD once a natural frequency match between the oscillating liquid column and the host structure is achieved. The oscillating fluid was considered to be water for all cases.

Table 6. TLCD parameters for simulation considering the full-scale structure and the experiment.

Property	Symbol	Full-scale Turbine	Small-scale Model
Weight of TLCD with water (kg)	M_d	2889	0.059
Damping Ratio of TLCD	ζ_d	0.063	0.0986
Length to column width ratio	α	0.7	0.3
Mass ratio	μ	0.02	0.05

The variation of natural frequency of the full-scale wind turbine tower for different soil-structure interaction scenarios are presented in Table 7.

Table 7. Natural frequency (Hz) of the full-scale wind turbine tower for a range of soil types.

Soil Type	Dry Sand	Saturated Sand	Clay
Natural frequency of fixed cantilever without mass of TLCD (Hz)	0.435	0.435	0.435
Natural frequency tower in soil without TLCD (Hz)	0.230	0.228	0.222
Natural frequency of fixed cantilever with added mass equivalent to that of the TLCD (Hz)	0.431	0.431	0.431
Natural frequency of tower in soil with added mass equivalent to that of the TLCD (Hz)	0.232	0.231	0.224

Since the natural frequency for a soft-soil type of this structure is suggested to be 0.25Hz, it seems reasonable to conclude that this method of calculating the natural frequency is reasonably accurate. The estimates for a small-scale model testing for different soil conditions are presented in Table 8.

Table 8. Natural frequency of the small-scale wind turbine tower for a range of soil types.

Soil Type	Sand	Top Soil	Clay
Natural frequency of fixed cantilever without mass of TLCD (Hz)	18.6	18.6	18.6
Natural frequency equivalent tower in soil without TLCD (Hz)	1.652	1.651	1.657
Natural frequency of fixed cantilever with added mass equivalent to that of the TLCD (Hz)	17.61	17.61	17.61
Natural frequency of equivalent tower in soil with added mass equivalent to that of the TLCD (Hz)	1.799	1.798	1.792

3.2 Parameter studies in the frequency domain

Parameter studies for the combined tower-soil-TLCD system was carried out in the frequency domain by plotting the transfer functions for different input scenarios. The transfer function of

the turbine without the TLCD is for an end mass equivalent to that of the TLCD without water and the nacelle combined, thus the natural frequency of the turbine changes as water is added. The TLCD is optimised for this new natural frequency. Different damping ratios have been used for the TLCD to examine the effects of damping once the natural frequency of the TLCD is tuned to that tower.

The effect of a tuned TLCD on the full-scale wind turbine is shown in Figure 2 for the three different soil conditions considered in this paper.

FIGURE 2 HERE

The results presented in Figure 2 demonstrate that a significant reduction in the magnitude of the structural response is achievable when an optimised TLCD is coupled with the structure for all these soil types. These graphs are for a structural damping ratio of 1%.

FIGURE 3 HERE

The variation in the percentage damping achieved by a TLCD is shown in Figure 3 for different structural and TLCD damping ratios, where ζ_s is the structural damping ratio and ζ_d is the damping ratio associated with the TLCD. This shows that even for a structural damping of 10% and TLCD damping ratio of 1%, there is still a small reduction in the magnitude of the structural response. However, unless vibrations are applied exactly at the natural frequency, it is unlikely that this small amount of damping will be worth the extra effort of installing a reasonably well-performing TLCD, so care should be taken when installing a TLCD to ensure that it is properly optimised to the natural frequency of the tower and that it has a reasonable level of damping.

The effect of a TLCD is also investigated for the experimental model and the results for individual soils are presented in Figure 4.

Similar to the results for the full-scale model, Figure 4 shows that considerable damping effect is possible to achieve with an optimised TLCD. It should be noted that the position of the double peak has moved slightly, due to the change in the mass ratio, which will be discussed later. As with the full-scale turbine, the effect of the TLCD on the structure is similar for all three soil types.

FIGURE 4 HERE

Figure 5 presents the effects of different structural and TLCD damping ratios, where ζ_s is the structural damping ratio and ζ_d is the damping ratio associated with the TLCD for the small-scale model.

FIGURE 5 HERE

The results demonstrates that a TLCD can reasonably reduce the magnitude of the structural response even when all parameters are not optimal as long as it is tuned, has some mass, and there is a reasonable amount of damping (Figure 5). Such reduction may be observed through small-scale experimentation. The effect of the changing length ratio becomes more significant as the damping ratio increases, indicating that the importance of ensuring a high length ratio increases as the damping of the TLCD is increased.

The investigation into the efficiency of TLCD for a small-scale experiment based on changes in mass ratio and length ratio is shown in Figure 6.

FIGURE 6 HERE

It is observed that the damping effect of the TLCD increases as the mass ratio increases. The improvement in damping achieved by increasing α remains similar for the different mass ratios, highlighting the importance of optimising both parameters. It should be noted that while a mass ratio of 10% is shown, a mass ratio of 5% is taken as optimal [13]. A mass ratio above 5% may lead to an excessive amount of mass to the top of the structure and therefore introduces the need for larger foundations. Similar to the effect of changing the damping ratio, the effect of increasing the length ratio becomes more pronounced as the mass ratio increases.

The effect of detuning of the TLCD is investigated in Figure 7.

FIGURE 7 HERE

It is observed that while the TLCD is most effective for a tuning ratio of 1, for a natural frequency of the TLCD less than that of the structure, the TLCD continues to reduce the response of the structure to a certain extent. When the tuning ratio is greater than one, the reduction in the effectiveness of the TLCD becomes more significant for a small change. As with the changes in the damping and frequency ratio, the effect of optimising the length is evident. Consequently, if the natural frequency of the wind turbine is expected to decrease over time due to damage to the structure or reduction in soil strength under cyclic loading conditions, starting with a tuning ratio slightly less than one may ensure that the TLCD continues to achieve a significant amount of damping over time. Alternatively, the TLCD could be re-tuned to the new natural frequency to ensure that it is performing as effectively as possible. One advantage of the TLCD is that recalibration is a relatively simple process for small changes in the natural

frequency, only requiring a change in the amount of water in the damper to change its natural frequency and improve its performance.

Considering the risk of damage to the structure, variations in soil characteristics under high cyclic loading conditions, discrepancies between calculations and on-site condition and the difficulties with fitting a installing a fully optimised TLCD, there is a possibility that a designed TLCD will not be fully optimised for the entire lifespan of the wind turbine. The numerical studies indicate that even under such circumstances, for a considerable range of non-optimised conditions and some amount of detuning, the TLCD can still effectively mitigate vibrations to a reasonable extent. This increases the viability of TLCDs for possible use even when there might be considerable uncertainty.

3.3 Demonstration of TLCDs in time domain

The response of the full-scale tower with and without a TLCD was numerically simulated in the time domain for a sinusoidal load (Figure 8), an impulse load (Figure 9), and for a broadband excitation in the form of Gaussian white noise (Figure 10). The sinusoidal load is applied at the natural frequency. The aim was to visualise the effectiveness of TLCDs for some fundamental signals which can be combined to create responses to any broadband time domain signal with random broadband and sinusoidal components, which is typical for wind loading. Both displacement and velocity are controlled due to TLCD.

FIGURE 8 HERE

FIGURE 9 HERE

FIGURE 10 HERE

3.4 Sensitivity to variations in input parameters

Sensitivity of some of the obtained results to variations in some relevant input parameters are investigated next for both full-scale and scaled conditions. Shear modulus of soils may vary depending on the scaling for a full-scale turbine or a small-scale experiment. The mass ratio (μ) and the length ratio (α) of the TLCD are critical since for practical applications these are the two factors that we have more control over and can vary. Sometimes, variation can also come from geometric constraints during application. The optimum damping ratio $\zeta_{opt} =$

$$\frac{\alpha}{2} \sqrt{\frac{2\mu(\alpha^2 \frac{\mu}{4} - \mu - 1)}{(\alpha^2 \mu^2 + \alpha^2 \mu - 4\mu - 2\mu^2 - 2)}} \text{ and optimum tuning ratio } \gamma_{opt} = \frac{\sqrt{1 + \mu(1 - \frac{\alpha^2}{2})}}{1 + \mu} \text{ can also thus see variation.}$$

The tower properties are usually fixed values dependent on the particular turbine for both full-scale or a scaled model. For a full-scale model, this section considers data from [25] and this is summarised in Table 9. The estimated damping of the primary system was $\zeta_s = 0.05$ keeping in mind that recommended values are usually between 0.02-0.08 [25] for operational wind turbines. The match of frequencies can be made closer by choosing and changing the damping ratios in this range. However, that leads to an ad-hoc reduction of error and the difference in estimated and measured frequencies for a mid-range damping ratio is presented here to highlight and establish typical levels of discrepancies that can be expected from such modelling. Additionally, the measured natural frequencies tend to vary over time, even due to thermal effects and as such an artificial matching of the two values by choosing the damping ratio conveniently does not serve any significant purpose.

Table 9. Comparison of Measured natural frequencies to those calculated by theoretical model using available tower properties from [25].

<i>Wind Farm Name</i>	<i>Country</i>	<i>Soil Conditions</i>	<i>Measured Natural Frequency (Hz)</i>	<i>Natural Frequency from Theoretical Model (Hz)</i>
<i>Lely Offshore Wind Farm</i>	<i>UK</i>	<i>Soft clay in the uppermost layer to dense and very dense sand layers below</i>	<i>0.634</i>	<i>0.475</i>
<i>Irene Vorrink Offshore Wind Farm</i>	<i>Netherlands</i>	<i>Soft layers of silt and clay in the upper seabed to dense sand and very dense sand below</i>	<i>0.546</i>	<i>0.465</i>
<i>Kentish Flats Offshore Wind Farm</i>	<i>UK</i>	<i>Layers of dense sand and firm clay</i>	<i>0.339</i>	<i>0.23</i>

To better understand the sensitivity of input parameters to final results for full-scale examples, tower properties from Lely Offshore Windfarm, as reported in [25] is used (Table 10). Small variations in soil properties do not change the results too much but the fundamental change in the type of soil does. Under these circumstances, a further choice of some varied soil properties are considered (Table 11) with description of the soils provided as a justification of their choice and to investigate their effects in the computed results. The changes in peaks of response functions $(H(w)_{\max})$ due to variations of parameters considered in this section is presented in Table 12 while the optimum tuning values for varying mass and length ratios are provided in Table 13.

Table 10. Lely offshore windfarm, tower properties from [25]

<i>Turbine Dimension Lely A2</i>	
<i>Structure height (m)</i>	50
<i>Tower top Diameter (m)</i>	1.9
<i>Tower bottom Diameter</i>	3.2
<i>Tower Wall Thickness (m)</i>	13.0
<i>Monopile Wall Thickness (m)</i>	35
<i>Nacelle Mass (m)</i>	32
<i>Young's Modulus Tower (Steel)(GPa)</i>	210
<i>Monopile Depth (m)</i>	13.5
<i>Shear Modulus of Soil G (MPa)</i>	140
<i>Measured Natural Frequency (Hz)</i>	0.634

484

485

486

487 Table 11. Shear Moduli used in investigating sensitivity computed peak value of frequency
 488 response of the tower structure in relation to soil properties and in the absence of TLCD

Shear Modulus of Soil (MPa)	H(w)_{max} No TLCD	Soil Description
<i>G=140</i>	<i>183.5</i>	<i>Soft clay in top layer. Dense to very dense sand layers below.</i>
<i>G=60</i>	<i>184.2</i>	<i>Layers of dense sand and firm clay</i>
<i>G=2150.5</i>	<i>181.9</i>	<i>Rocky seabed (weathered bedrock)</i>

489

Table 12. Peak value of frequency response with varying shear moduli, length ratios and mass ratios in percentage (μ)

μ (%)	$H(w)_{max}$								
	$\alpha = 0.1$			$\alpha = 0.5$			$\alpha = 0.9$		
	$G=140$ <i>Mpa</i>	$G=60$ <i>Mpa</i>	$G=2150.5$ <i>Mpa</i>	$G=140$ <i>Mpa</i>	$G=60$ <i>Mpa</i>	$G=2150.5$ <i>Mpa</i>	$G=140$ <i>Mpa</i>	$G=60$ <i>Mpa</i>	$G=2150.5$ <i>Mpa</i>
0.5	46.28	43.03	43.10	38.45	38.46	38.42	34.74	34.76	34.70
1	42.90	42.94	42.81	35.82	35.85	35.76	31.43	31.45	31.39
5	44.04	44.05	44.04	30.12	30.14	30.09	24.01	24.01	24.00
10	46.34	46.38	46.27	28.77	28.77	28.75	22.00	22.01	21.99

Table 13. Optimum damping and tuning ratios with varying length and mass ratios in percentage (μ).

μ %	$\alpha = 0.1$		$\alpha = 0.5$		$\alpha = 0.9$	
	ζ_{opt}	γ_{opt}	ζ_{opt}	γ_{opt}	ζ_{opt}	γ_{opt}
0.5%	0.004	0.997	0.018	0.997	0.032	0.997
1%	0.005	0.995	0.025	0.994	0.045	0.993
5%	0.011	0.976	0.055	0.973	0.099	0.966
10%	0.015	0.953	0.076	0.948	0.137	0.936

The variations in frequency response functions for the base-case but with changing length ratios are presented in Figure 11, the effects of changing mass ratios in Figure 12 and for different soil types in Figure 13.

FIGURE 11 HERE.

FIGURE 12 HERE.

FIGURE 13 HERE.

A similar study was carried out for the small-scale model as well. Table 14 provides the variations considered in shear moduli and the corresponding changes in the peak frequency response magnitude, without TLCD and with an assumed damping ratio $\zeta_s = 0.01$ while Table 15 provides the properties of the corresponding scaled-down tower. The maximum frequency response magnitudes for variations in shear moduli of soil with length and mass ratios are presented in Table 16 while the optimum damping and tuning ratios for varying length and mass ratios for TLCD is presented in Table 17.

Table 14 Shear Moduli from small-scale experiment for sensitivity analysis of soil properties

<i>Shear Modulus of Soil G (MPa)</i>	<i>H(w)_{max}</i>	<i>Soil Description</i>
12.72	3.672	Dry Sand
8	3.672	Soil (assumed)
2	3.672	Kaolin Clay

Table 15. Scaled-down tower properties for analysing sensitivity to inputs for small-scale experiments.

<i>Turbine Dimension</i>	<i>Small-scale Turbine</i>
<i>Structure height (m)</i>	1.2
<i>Tower Diameter (m)</i>	0.04
<i>Tower Wall Thickness (m)</i>	0.002
<i>Monopile Wall Thickness (m)</i>	35
<i>Nacelle Mass (kg)</i>	0.9
<i>Young's Modulus Tower (Aluminium) (Gpa)</i>	69
<i>Monopile Depth (m)</i>	0.3

515 Table 16. peak value of frequency response with varying shear moduli, length ratios and mass
516 ratios in percentage (μ) for scaled experiments.

μ (%)	$H(w)_{max}$								
	$\alpha = 0.1$			$\alpha = 0.5$			$\alpha = 0.9$		
	<i>Sand</i>	<i>Soil</i>	<i>Clay</i>	<i>Sand</i>	<i>Soil</i>	<i>Clay</i>	<i>Sand</i>	<i>Soil</i>	<i>Clay</i>
0.5	2.69	2.64	2.38	1.55	1.54	1.49	1.23	1.23	1.23
1	2.40	2.43	2.54	1.35	1.35	1.34	0.96	0.96	0.94
5	1.93	2.00	2.18	0.86	0.85	0.84	0.59	0.59	0.58
10	2.06	2.13	2.17	0.78	0.78	0.77	0.52	0.52	0.52

517
518 Table 17. Optimum damping and tuning ratios with varying length and mass ratios in percentage
519 (μ)

μ %	$\alpha = 0.1$		$\alpha = 0.5$		$\alpha = 0.9$	
	ξ_{opt}	γ_{opt}	ξ_{opt}	γ_{opt}	ξ_{opt}	γ_{opt}
0.5	0.004	0.997	0.018	0.997	0.032	0.997
1	0.005	0.995	0.025	0.994	0.045	0.993
5	0.011	0.976	0.055	0.973	0.099	0.966
10	0.015	0.953	0.076	0.948	0.137	0.936

520
521 The variations in frequency response functions for the small-scale models with changing length
522 ratios are presented in Figure 14, the effects of changing mass ratios in Figure 15 and for
523 different soil types in Figure 16.

524 **FIGURE 14 HERE.**

525 **FIGURE 15 HERE.**

526 **FIGURE 16 HERE.**

Parameter studies around other secondary effects have been observed recently to be of importance in terms of design efficient performance during operational lifetime [26, 27].

5 EXPERIMENTAL SET-UP FOR SMALL-SCALE LABORATORY EXPERIMENTATION

A small-scale experimental study was subsequently carried out in a laboratory to investigate and demonstrate the use of TLCD for vibration control of a wind turbine tower considering soil-structure interaction.

5.1 Experimental considerations for alignment with numerical investigation

The tuning ratio $\gamma = \frac{\omega_d}{\omega_s}$ changes with the change in the length of liquid in the column in a TLCD and provides the best vibration mitigation when equal to 1. This can be controlled in the laboratory by changing the water levels in the TLCD. The optimum length of liquid column for maximum damping of the system is related to the natural frequency of the primary system and relationship is expressed as $\sqrt{2g/L_d}$. As the liquid is added however, the natural frequency of the system will decrease slightly due to the change of the mass of the entire system, therefore affecting the optimum length of column of liquid to a certain extent. With a pipe diameter chosen for the TLCD, it is also possible to determine the amount of water in *ml* ($10^{-3}l$), corresponding to the length of column of water. Yalla and Kareem [13] determined that the greatest damping was achieved for a mass ratio of approximately 5% of the primary structure, but also showed that the TLCD is still effective for a mass ratio as low as 0.5%. Another important parameter is the ratio of horizontal length to liquid column (α). If the ratio is 1.0 then

the control system effectively acts as a TMD. The optimum head-loss coefficient, determined by size of orifice was investigated by Yalla and Kareem [13] and it was found that for lower amplitudes of excitation, higher vibration mitigation was achieved by constricting the liquid flow through the orifice and at higher amplitudes, opening of the orifice and higher liquid velocity contributed to the appropriate level of damping. The soil-structure interaction acts as a set of lateral springs at the base of the turbine and it is important to model the effect the soil has on the natural frequency of the system and on the dynamics of the excited beam [19]. To simplify the model, it will be assumed that the bearing capacity of the soil is sufficient to prevent any axial displacement, hence only rotational and lateral displacement need be considered. In order to eliminate grain size effect in scaling, it is necessary for the ratio between the average grain size and the pile diameter, to be larger than 88 [24]. In line with experiments performed for offshore wind turbines by Bhattacharya and Adhikari [19] and Bhattacharya et al. [23], the model dimensions will be at a 1:100 scale.

5.2 Experimental parameters and boundary conditions

To establish the optimum length of column of liquid in the TLCD, experiments started without any liquid in the TLCD, so that the original natural frequency of the beam-soil system can be estimated experimentally. Next, an amount of liquid, well below what is required for the TLCD to be tuned, was added. This procedure was then repeated, gradually increasing at 0.015l amounts until nearing the optimum level where the incremented amounts should be reduced to 0.005l and 0.002l amounts until the optimum has been passed and then return to 0.015l additions. Two orifices of 0.012m and 0.008m were chosen for the experiment to observe the effect on the damping of the TLCD by varying the head-loss coefficient.

The varying length of column of water will affect the length ratio since the horizontal length is not variable for this specific application due to geometric constraints. A pipe diameter of $0.020m$ ($0.016m$ inside diameter) was chosen and this choice was guided by the mass ratio of TLCD to primary system where the primary system had a mass of $\sim 750g$ (above the surface of the soil) and the mass ratio sought being 5%, [13].

The geometry of the turbine was kept constant while the material used for the beam was aluminium. The TLCD was attached to the structure using two clamps. Accelerometers were secured to the test turbine using a number of cable ties.

The soils chosen for this experiment are: kaolin (fine grained clay), top soil, and sand. Each of these has their unique properties and will have an effect on the damping of the scaled tower and the natural frequency of the combined soil-structure-TLCD system.

5.3 Experimental Set-up

The TLCD and primary system were set up connected to a permanent magnet shaker where the excitation was transferred to the turbine through a probe. White noise was applied to the test structure for using this setup. Additionally, an impulse excitation was applied to the structure using a pendulum with the mass of the pendulum swinging from a height and impacting the turbine. The height of the falling mass and the location was kept the same each time to obtain control over the repeatability of input impulse force for each experiment. The weight used as a pendulum was a stainless-steel eye bolt with a mass of $0.068kg$. The pendulum string was $0.345m$ in length and the angle to the turbine from which it was released being 44° . The pendulum was caught after each hit, ensuring that it did not interfere with the response of the

system after the initial impact. In order to obtain consistent values for the response and acceleration of the system, each test included a sequence of 10 hits with a 10 second break (to allow the system to return to equilibrium). The soil was repacked after every sequence of hits to ensure consistence of the soil conditions.

An X-Bee Wasmote 3D accelerometer, consisting of a Wasmote board, an X-Bee Series 2 radio, an SD card and a battery pack was connected near the top of the model turbine tower (Figure 17). The co-ordinator had an X-bee PRO radio. The accelerometer was attached to the turbine with cable ties. Sensor deployment [28] and the effective energy demand management of sensors [29] remain a challenging communications problem in this field for full scale deployment, but small-scale experiments can be helpful in providing insights for such implementation and act as a test-bed for assessing methods and algorithms.

FIGURE 17 HERE

The model TLCD was designed to accommodate some changes in its natural frequency with a water column. The two critical parameters in the design were the mass-ratio and the length ratio, which has also recently been observed to be key in preliminary tests reported on floating platforms with TLCD [30]. A 0.02m pipe was chosen for the TLCD with an inside diameter of 0.016m with corner connections so that different vertical lengths and orifice sizes could be interchanged (Figure 18).

FIGURE 18 HERE

A diameter of 0.030m was chosen for the model tower made of an aluminium beam. Holes were made in the beam for the attachment to the actuator (later used to attach the pendulum) and for

clamps to keep the TLCD fixed to the beam. The Beam was also designed to facilitate the inclusion of a mass on top, for the possibility of a modelled nacelle. A schematic diagram of the wind turbine supported on a monopole is shown in Figure 19.

FIGURE 19 HERE

Table 18 provides the dimensions of the apparatus required for experimentation. At the optimal length of column of water with the above dimensions equate to a length ratio of 0.287. The soil was placed in a 7l tub of 0.45m height and 0.480m diameter.

Table 18. Experimental dimensions for small-scale testing performed in laboratory.

Unit Element	Mass (kg)	System	Element	Dimension (m)
Full Assembly	1.281	Turbine Beam	Height	1.500
Accelerometer	0.173		Diameter	0.035
TLCD + Clamps	0.103		Thickness	0.0045
Turbine Beam	1.005	TLCD	Horizontal Length (<i>b</i>)	0.08
Beam above soil	0.804		Vertical Height	0.2
Beam Below soil	0.201		Full Length of Column (<i>l</i>)	0.48
System Above Soil	1.080		Diameter	0.02
Pendulum	0.068		Internal Diameter	0.016
		Orifices	Small	0.008
			Large	0.012

The data was recorded at a sampling rate of 50Hz to reasonably accommodate frequencies as high as 15Hz while the estimated natural frequency was around 10Hz. The accelerometer writes data to its own SD card, which was subsequently written to a csv file. Time was allowed between each impulse to allow the system to return to rest. To have a better confidence on testing, two different orifice diameters and two different accelerometers were used and it was

ensured that there was no significant change in the variability of data and the observed phenomena.

6 EXPERIMENTAL RESULTS

Frequency domain graphs of the system under impulse excitation are presented for both 0.012m orifice and 0.008m orifice. Figure 20 presents a frequency domain representation of how the response amplitudes change as the water column in TLCD approaches the natural frequency of the structure. The top soil is chosen as the experimental soil as it is representative of a state between sand and clay (kaolin).

FIGURE 20 HERE

With no water in the TLCD, the optimum length of column of water in the TLCD for a natural frequency of 8.4Hz is 0.278m which for a 0.016m internal diameter of pipe equates to an optimum volume of 0.056l of water, which is approximately 5.2% of the mass of the primary structure above the level of the soil. The experimentation matched this calculated figure, as the lowest response observed was with 0.056l of water in the TLCD. For tuned condition, this reduction of tower vibration is presented in the frequency domain in Figure 20.

FIGURE 20 HERE

As the volume of liquid is increased, the amplitude of the frequency response of the structure to the applied loading decreases 6.8 to a minimum of 3.5, which is a 48.5% reduction. However, as the volume of liquid was increased past the optimum, the response amplitude in the frequency

646 domain increased again to a maximum of 6.2 at 0.07l of water, something that might be
647 expected when the TLCD is tuned significantly away from the natural frequency of the tower.

648 The level of response is significantly sensitive to the change in length of column/volume of
649 water around the optimum value. With an increase of 0.001l, from 0.055l to 0.056l, the response
650 amplitude in the frequency domain dropped significantly from 4.5 to 3.5. When this optimum
651 volume of 0.056l was surpassed, the response quickly returned to 4.3 after an addition of 0.001l.
652 Consequently, the best reduction in vibration for a TLCD is valid for a relatively short domain of
653 frequency range and TLCDs must be retuned over the life span of such structures. The increase
654 in response after passing the optimum was far quicker, in terms of volume of liquid added, than
655 that of the increase towards the optimum. By the time 0.061l was added in the column, the
656 amplitude of the frequency response had returned to 6.

657 An interesting observation was that when the volume of water was increased to 0.085l, the
658 response function returned from 6.1 to 5. This is due to the fact that 0.085l of water equates to
659 around 8% of the mass of the tower structure and some additional damping could be leveraged
660 from this significantly higher volume of water leading to a longer column length. However, for
661 practical design purposes, it is not advisable to load the tower with significantly high mass and
662 this mass ratio is not a feasible value for deployment.

663 For actual deployment, the constrained tower dimensions can prove problematic for TLCDs.
664 Issues arise when optimising the length ratio. Providing a sufficient length of column, so that the
665 TLCD can be tuned to the natural frequency of the wind turbine, can sometimes be difficult.
666 While this paper has focused on a uniform, U-shaped TLCD other effective shapes can also be
667 investigated, including alternatives like S-shaped TLCD [31], which is mainly designed for a

primary system with restricted horizontal length. Ideally, TLCD could be located within the turbine nacelle. However, there can be space issue in the nacelle for an effective TLCD, even when considering a mass ratio as low as 2%. On the other hand, a TLCD located outside the nacelle can complicate the dynamics of the combined system by itself vibrating due to wind effects. A TLCD located within the nacelle, near to the boundaries may be of interest in this regard, which would address these problems. A study found that that increasing the cross-sectional area ratio of the TLCD could greatly reduce the length requirement, compared to that of a TLCD with a uniform cross-section in suppressing the same level of structural vibration [32]. Yalla and Kareem [13] investigated the use of multiple TLCDs and demonstrated the performance of MTLCDs in controlling multiple modes under wind excitation and this has also been recently observed for floating platforms. This can be another option to investigate. For the nacelle, the majority of the primary mechanisms are the located at the centre of the nacelle, with the rest being additions, whose specific location is not generally as critical. These could be reorganised to make geometrical space for practical deployments of TLCDs. Locating two TLCDs in the nacelle, one on each side of the generator and the shaft can be useful in this regard. Both will be integrated into the nacelle and have a reduced horizontal cross-sectional area, which will reduce the required tuning length and not require the same amount of vertical space as a uniform TLCD would. One more option is on the side of monitoring of renewable energy devices and platforms, the need for which is being increasingly felt [33]. With diverse and novel output-only real-time methods [34] and markers [35] available for structural health monitoring, it is expected that these methods can eventually help tracking and identifying changes and impacts of implementation of passive control options and possible variations in tuning [1]. Finally, recent works on extreme value analyses for structural health monitoring [36]

indicate that such aspects can be relevant and applicable to tracking and marking performance of deployed TLCDs.

7 CONCLUSIONS

This paper presents a study on TLCDs deployed to control vibrations of wind turbine towers while considering the interaction of the tower and the foundation soil. A theoretical framework is created first to integrate the soil-structure interaction of the tower with the aspect of passive control via TLCDs. Subsequently, numerical investigation is carried out to understand the effect of soil-structure interaction on the control of wind turbine towers using TLCD. Quantitative estimates of the key governing parameters on such design are obtained. The theoretical framework, along with some scaling consideration is used to design a small-scale experiment to validate the theoretical observations qualitatively. Experiments are carried out to illustrate the numerical findings. It was found that soil-structure interaction play a key role is designing TLCD for wind turbine tower vibration control and the optimal tuning of the TLCD may need re-adjustment over the life-span of the turbines. TLCDs were observed to be a viable method of wind turbine tower vibration control. The optimal mass and the tuning of the TLCD with the natural frequency of the tower after considering soil-structure interaction were observed to be the main factors for design of TLCD to obtain a reasonably good performance. Variations in other parameters can take place to a certain extent without affecting the performance of TLCD significantly. Even when detuned, TLCDs can reasonably work but the peak performance is easily affected by small amounts of detuning. Consequently, re-adjustment of TLCD liquid length is suggested if maximised performance of TLCDs is expected at all levels. An

experimental framework was devised and successfully applied to observe such theoretical predictions within a laboratory framework. The integrated numerical framework and numerical experimentation may be extended to assess TLCD control in future with variations in TLCD design and for other soil or structural conditions. The framework is useful for assessing variations in design of wind turbines and in choosing and understanding other control strategies as well, where soil-structure interaction can play an important role.

Acknowledgement

This research was supported by Science Foundation Ireland (SFI) Centre MaREI - Centre for Marine and Renewable Energy (12/RC/2302).

References

1. Arrigan, J., V. Pakrashi, B. Basu, and S. Nagarajaiah, *Control of flapwise vibrations in wind turbine blades using semi-active tuned mass dampers*. Structural Control and Health Monitoring, 2011. **18**(8): p. 840-851.
2. Namik, H., and Stol, K, *Individual blade pitch control of floating offshore wind turbines*. Wind Energy, 2010. **13**: p. 74-85.
3. Liu, X., Bo, L., and Luo. H, *Dynamical measurement system for wind turbine fatigue load*. Renewable Energy, 2016. **86**: p. 909-921.
4. Jianu, O., M.A. Rosen, and G. Naterer, *Noise Pollution Prevention in Wind Turbines: Status and Recent Advances*. Sustainability, 2012. **4**(6): p. 1104.

- 733 5. Zhang, Z., S. Nielsen, F. Blaabjerg, and D. Zhou, *Dynamics and Control of Lateral*
734 *Tower Vibrations in Offshore Wind Turbines by Means of Active Generator Torque.*
735 *Energies*, 2014. **7**(11): p. 7746.
- 736 6. Murtagh, P., A. Ghosh, B. Basu, and B. Broderick, *Passive control of wind turbine*
737 *vibrations including blade/tower interaction and rotationally sampled turbulence.* *Wind*
738 *Energy*, 2008. **11**(4): p. 305-317.
- 739 7. Kumar, R.A., C.-H. Sohn, and B.H. Gowda, *Passive control of vortex-induced*
740 *vibrations: an overview.* *Recent Patents on Mechanical Engineering*, 2008. **1**(1): p. 1-11.
- 741 8. Lackner, M.A. and M.A. Rotea, *Passive structural control of offshore wind turbines.*
742 *Wind Energy*, 2011. **14**(3): p. 373-388.
- 743 9. Karimi, H.R., M. Zapateiro, and L. Ningsu. *Semiactive vibration control of offshore wind*
744 *turbine towers with tuned liquid column dampers using H_{∞} output*
745 *feedback control.* in *Control Applications (CCA), 2010 IEEE International Conference*
746 *on.* 2010.
- 747 10. Caterino, N., C. Georgakis, F. Trinchillo, and A. Occhiuzzi, *A semi-active control system*
748 *for wind turbines,* in *Wind Turbine Control and Monitoring.* 2014, Springer. p. 375-407.
- 749 11. Luo, N., Y. Vidal, and L. Acho, *Wind Turbine Control and Monitoring.* 2014: Springer.
- 750 12. Quilligan, A., O'Connor, A., and Pakrashi, V. *Fragility Analysis of Steel and Concrete*
751 *Wind Turbine Towers.* *Engineering Structures*, 2012. **36**: p. 270-282.

13. Yalla, S. and A. Kareem, *Optimum Absorber Parameters for Tuned Liquid Column Dampers*. Journal of Structural Engineering, 2000. **126**(8): p. 906-915.
14. Jaksic, V., C. Wright, A. Chanayil, S.F. Ali, J. Murphy, and V. Pakrashi, *Performance of a Single Liquid Column Damper for the Control of Dynamic Responses of a Tension Leg Platform*. Journal of Physics: Conference Series, 2015. **628**(1): p. 012058.
15. Jaksic, V., C.S. Wright, J. Murphy, C. Afeef, S.F. Ali, D.P. Mandic, and V. Pakrashi, *Dynamic response mitigation of floating wind turbine platforms using tuned liquid column dampers*. Phil. Trans. R. Soc. A, 2015. **373**: **20140079**(2035).
16. Damagaard, M., Zania, V., Andersen, L.V., and Ibsen, L.B., *Effects of soil–structure interaction on real time dynamic response of offshore wind turbines on monopiles*. Engineering structures, 2014. **75**: p. 388-401.
17. Lombardi, D., S. Bhattacharya, and D.M. Wood, *Dynamic soil–structure interaction of monopile supported wind turbines in cohesive soil*. Soil Dynamics and Earthquake Engineering, 2013. **49**: p. 165-180.
18. Zaaijer, M., T. Subroto, L. Speet, J. Vugts, R.v. Rooij, M.v.d. Kraan, S. Kay, B. Smith, U. Mirza, and P. Heywood, *Design Methods for Offshore Wind Turbines at Exposed Sites (OWTES); Sensitivity Analysis for Foundations of Offshore Wind Turbines (OWTES Task 4.1 OWEC Tools Task B.1 - B.2)*. 2002, Delft University of Technology, Section Wind Energy Delft, Netherlands

- 771 19. Adhikari, S. and S. Bhattacharya, *Vibrations of wind-turbines considering soil-structure*
772 *interaction*. Wind and Structures, 2011. **14**(2): p. 85.
- 773 20. van der Tempel, J. and D.-P. Molenaar, *Wind turbine structural dynamics-a review of the*
774 *principles for modern power generation, onshore and offshore*. Wind engineering, 2002.
775 **26**(4): p. 211-222.
- 776 21. Hartog, D.J.P., *Mechanical vibrations*. 4th edition ed. 1956, New York: McGraw-Hill.
- 777 22. Sakai, F. and S. Takaeda, *Tuned Liquid Column Damper - New Type Device for*
778 *Suppression of Building Vibrations*, in *Proceedings International Conference on High*
779 *Rise Buildings*. 1989: Nanjing, China.
- 780 23. Bhattacharya, S. and S. Adhikari, *Experimental validation of soil–structure interaction of*
781 *offshore wind turbines*. Soil Dynamics and Earthquake Engineering, 2011. **31**(5): p. 805-
782 816.
- 783 24. Klinkvort, R.T., C.T. Leth, and O. Hededal. *Centrifuge modelling of monopiles in dense*
784 *sand at The Technical University of Denmark*. in *Eurofuge 2012, Delft, The Netherlands,*
785 *April 23-24, 2012*. 2012. Delft University of Technology and Deltares.
- 786 25. Arany, L., Bhattacharya, S., Adhikari, S., McDonald, J.H.G. and Hogan, S.J. (2016), *Closed*
787 *form solution of eigen frequency of monopile supported offshore wind turbines in deeper*
788 *waters stiffness of substructure and SSI*. Soil Dynamics and Foundation Engineering
789 Vol.83, 18-32.

- 790 26. Wright CS, Pakrashi V and Murphy J. (2016). *The Dynamics Effects of Marine Growth*
791 *on a Point Absorbing Wave Energy Converter*, Offshore Energy and Storage Symposium
792 OSES 2016, Valletta, Malta.
- 793 27. Wright CS, Pakrashi V and Murphy J. (2016). *Dynamic Effects of Anchor Positional*
794 *Tolerance on Tension Moored Floating Wind Turbine*. Journal of Physics, Conference
795 Series, 753(9), 092019, 1-9
- 796 28. O'Donnell D, Srbinovsky B, Murphy J, Popovici E and Pakrashi V. (2015). *Sensor*
797 *Measurement Strategies for Monitoring Offshore Wind and Wave Energy Devices*.
798 Institute of Physics, Journal of Physics, Conference Series, 628(1), 012117-1-8.
- 799 29. Srbinovski B, Magno M, Edwards Murphy F, Pakrashi V and Popovici E. (2016). *An Energy*
800 *Aware Adaptive Sampling Algorithm for Energy Harvesting WSN with Energy Hungry*
801 *Sensors*. Sensors, 16(4), 448, 1-19
- 802 30. O'Donnell D, Murphy J, Desmond C, Jaksic V and Pakrashi V. (2017). Tuned Liquid
803 Column Damper based Reduction of Dynamic Responses of Scaled Offshore Platforms
804 in Different Ocean Wave Basins. Journal of Physics, Conference Series, 842, 012043.
- 805 31. Zeng, X., Y. Yu, L. Zhang, Q. Liu, and H. Wu, *A New Energy-Absorbing Device for*
806 *Motion Suppression in Deep-Sea Floating Platforms*. Energies, 2014. **8**(1): p. 111.
- 807 32. Gao, H., K.C.S. Kwok, and B. Samali, *Optimization of tuned liquid column dampers*.
808 Engineering Structures, 1997. **19**(6): p. 476-486.

- 809 33. Jaksic V, O'Shea R, Cahill P, Murphy J, Mandic DP and Pakrashi V. (2015). *Dynamic*
810 *Response Signatures of a Scaled Model Platform for Floating Wind Turbines in an*
811 *Ocean Wave Basin*. Philosophical Transactions of the Royal Society A: Mathematical,
812 Physical and Engineering Sciences, 373 (2035):20140078:1-20140078:18.
- 813 34. Krishnan M, Bhowmik B, Hazra B and Pakrashi V. (2018). *Real time damage detection*
814 *using recursive principal components and time varying autoregressive modeling*.
815 Mechanical Systems and Signal Processing, 101, 549-574.
- 816 35. Jaksic V, Mandic DP, Ryan K, Basu B and Pakrashi V. (2016). *A Comprehensive Study*
817 *of the Delay Vector Variance Method for Quantification of Nonlinearity in Dynamical*
818 *Systems*. Royal Society Open Science, 2, 150493-1-24.
- 819 36. Pakrashi V, Fitzgerald P, O'Leary M, Jaksic V, Ryan K and Basu B. (2018). *Assessment*
820 *of Structural Nonlinearities Employing Extremes of Dynamic Responses*. Journal of
821 Vibration and Control, Ahead of Print, DOI: 10.1177/1077546316635935

822

823 **List of Figures**

824 **Figure 1** An idealised model of a wind turbine tower considering soil-structure interaction.

825 **Figure 2** Transfer functions for full-scale wind turbine tower for different soils.

826 **Figure 3** Transfer function for different Structural and TLCD damping ratios for Dry Sand

827 **Figure 4** Frequency Response Functions of for Model Wind Turbine, Individual Soils

828 **Figure 5** Frequency Response Functions for Small-scale Model - Different TLCD
829 Damping and Length Ratio

830 **Figure 6** Frequency Response Functions for small-scale model considering different TLCD
831 mass and length ratio.

832 **Figure 7** Frequency Response Functions for an experimental model with varying tuning
833 ratio for a 5% mass ratio.

834 **Figure 8** Displacement and velocity responses of tower tip with and without TLCD for a
835 sinusoidal excitation at the tip equal to the natural frequency of the tower.

836 **Figure 9** Displacement and velocity responses of tower tip with and without TLCD for an
837 impulse excitation at the tip of the tower.

838 **Figure 10** Displacement and velocity responses of tower tip with and without TLCD for a
839 Gaussian white noise excitation at the tip of the tower.

840 **Figure 11** Variations of Frequency Response Functions due to changing length ratios.

841 **Figure 12** Variations of Frequency Response Functions for changing Mass Ratios.

842 **Figure 13** Variations of Frequency Response Functions for changing soil types for TLCD

843 Length Ratio of 0.9 and Mass Ratio of 0.05

844 **Figure 14** Variations of Frequency Response Functions in a scaled model on sand for varying

845 Length Ratios for Mass Ratio of 0.05.

846 **Figure 15** Variations of Frequency Response Functions in a scaled model on sand for varying

847 Mass Ratios with Length Ratio of 0.5.

848 **Figure 16** Variations of Frequency Response Functions in a scaled model on varying Soil Types,

849 with Mass Ratio of 0.05 and Length Ratio of 0.5.

850 **Figure 17** Wireless 3D accelerometer a) attached to turbine b) by itself c) components of

851 model TLCD

852 **Figure 18** Experiment setup for small-scale test: a) Schematic b) Image

853 **Figure 19** Experiments for top soil with varying water column length

854 **Figure 20** Experiments for top soil with a 0.012l orifice for TLCD comparing controlled and

855 uncontrolled situations

856

857

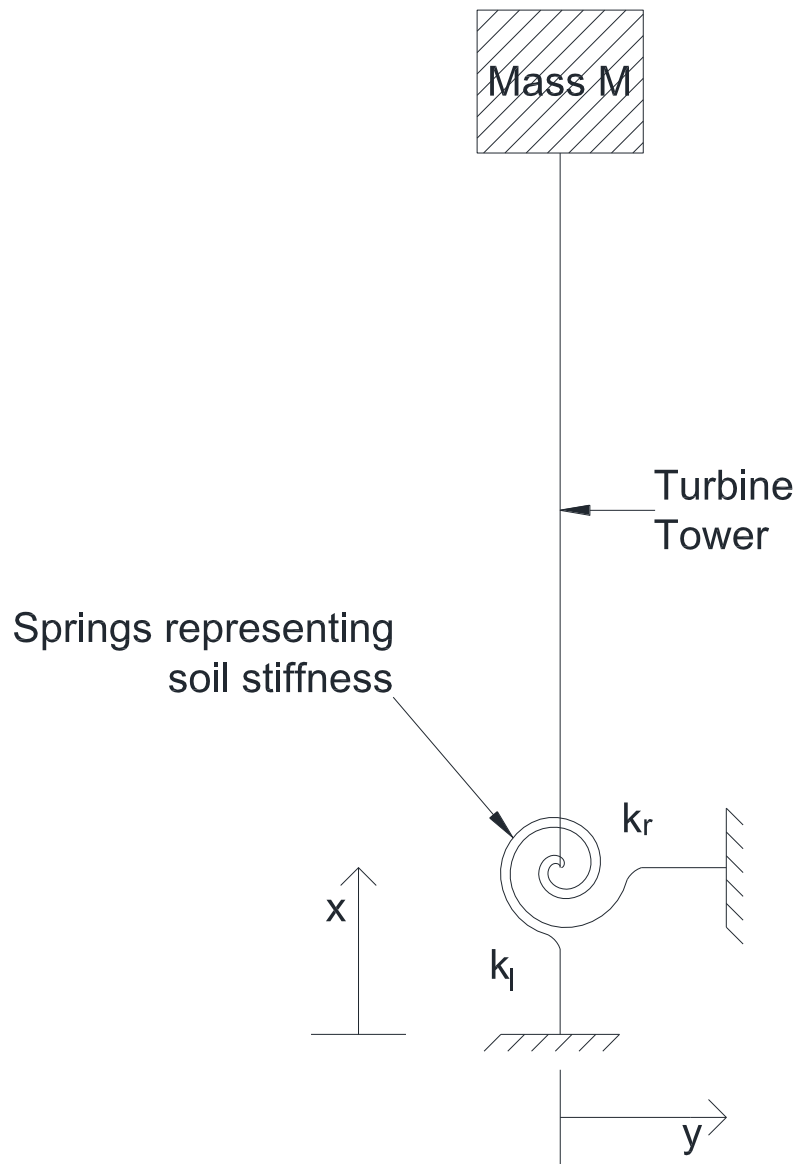


Figure 1

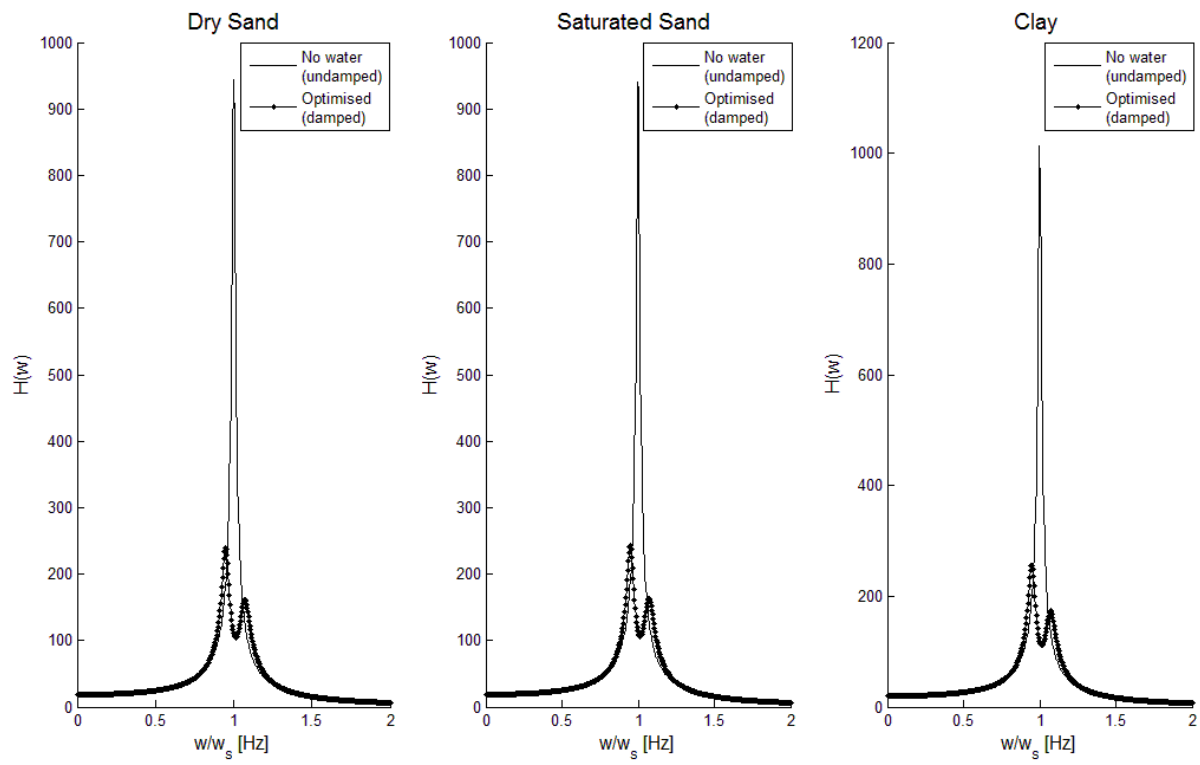


Figure 2

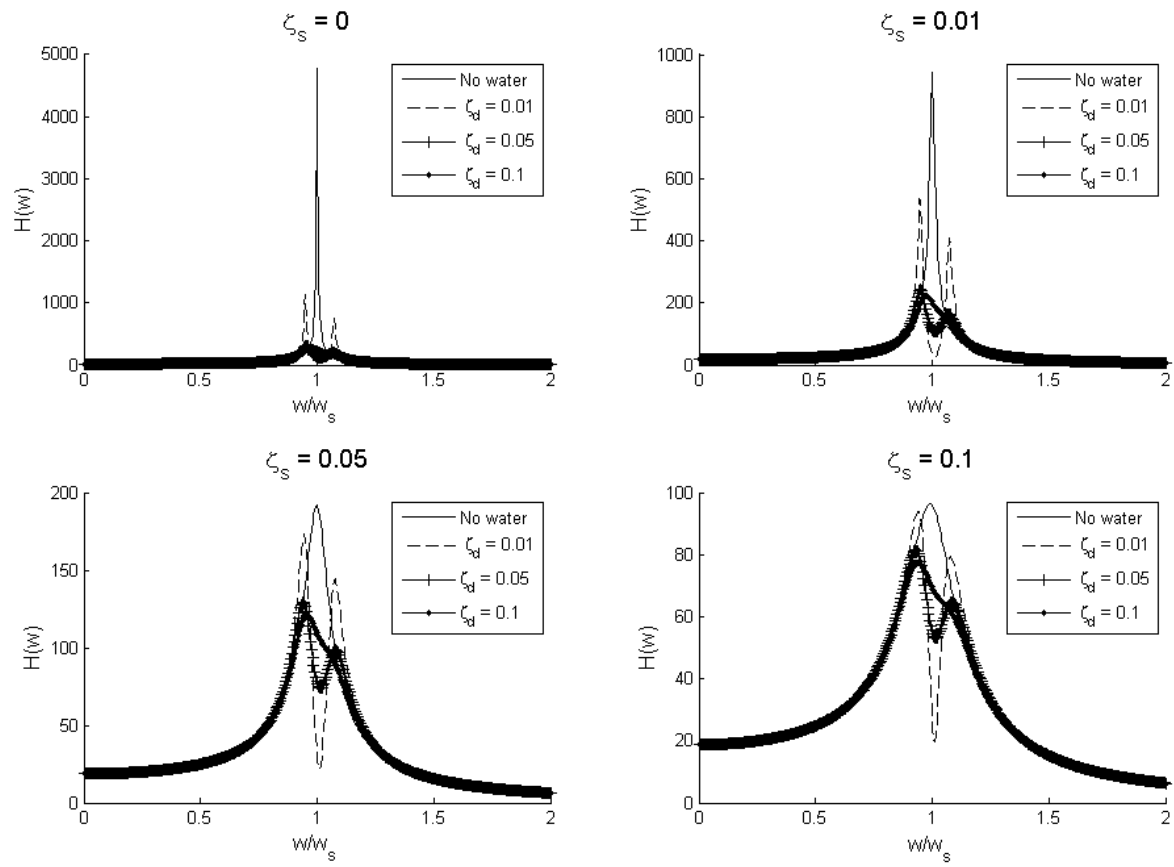


Figure 3

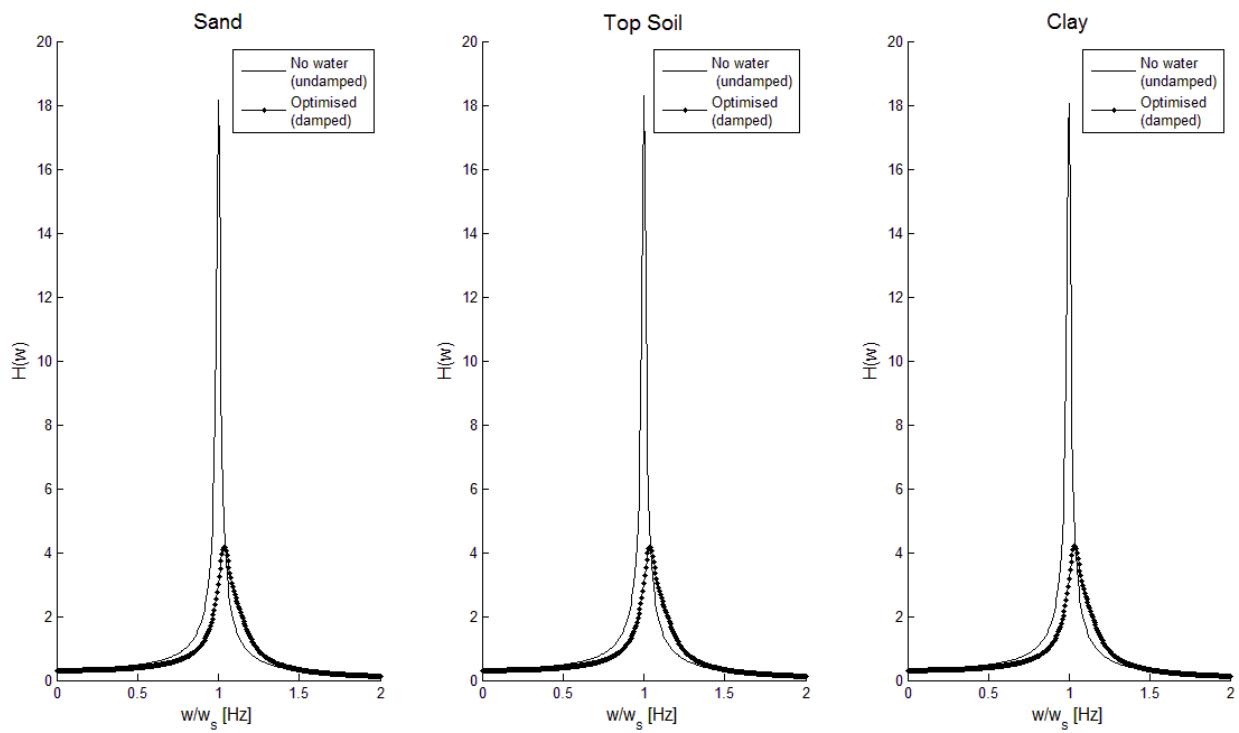


Figure 4

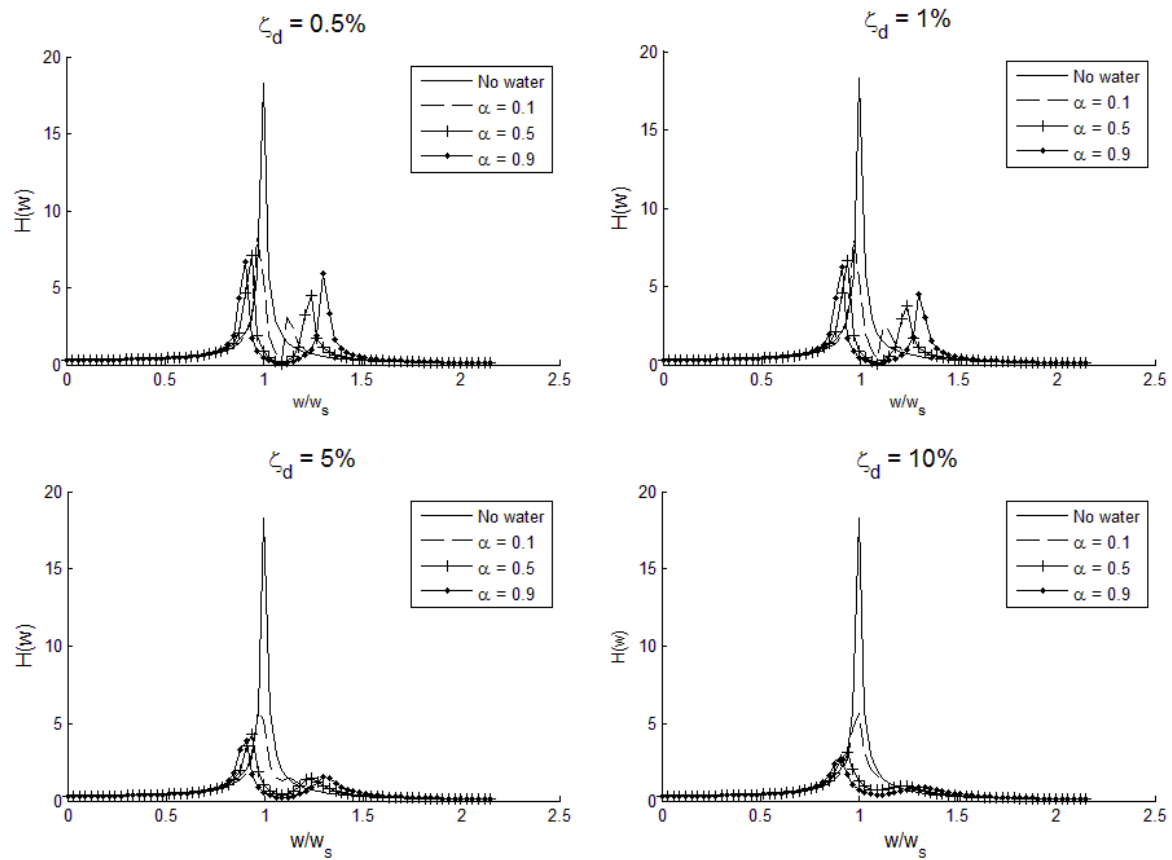


Figure 5

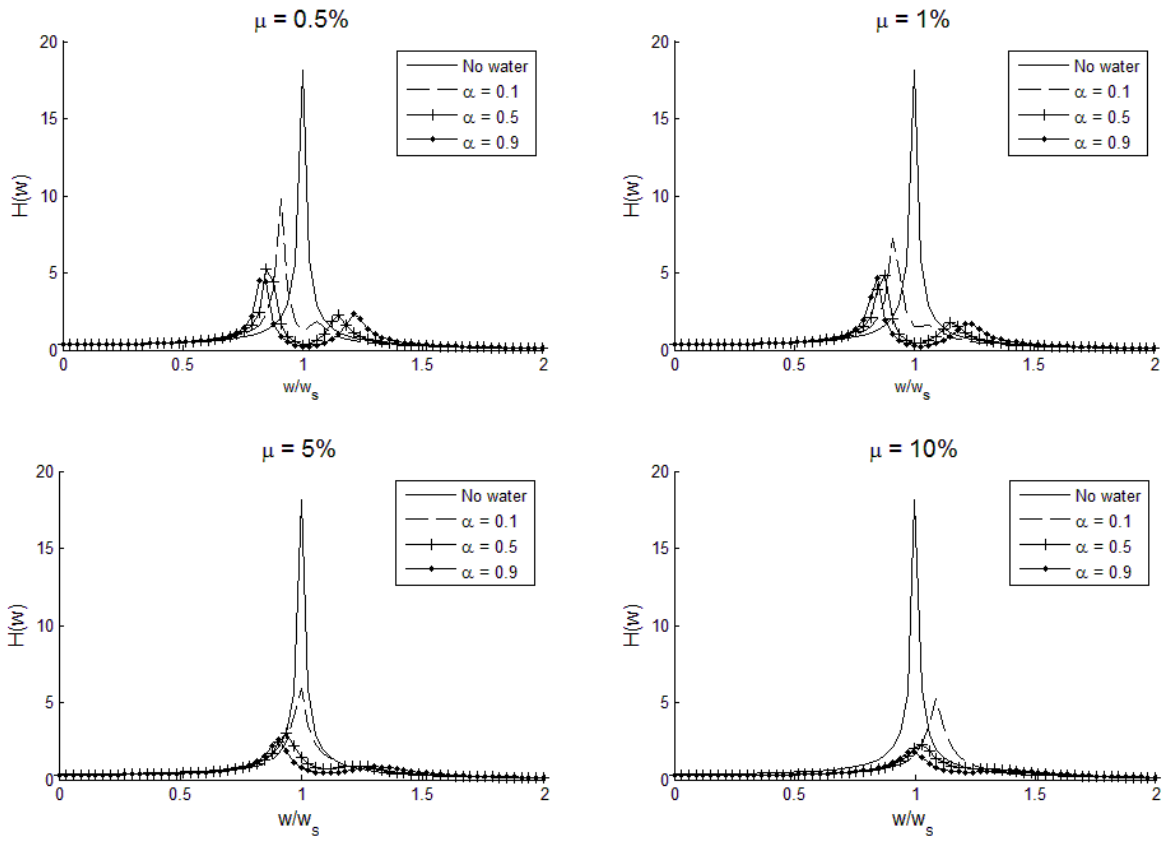


Figure 6

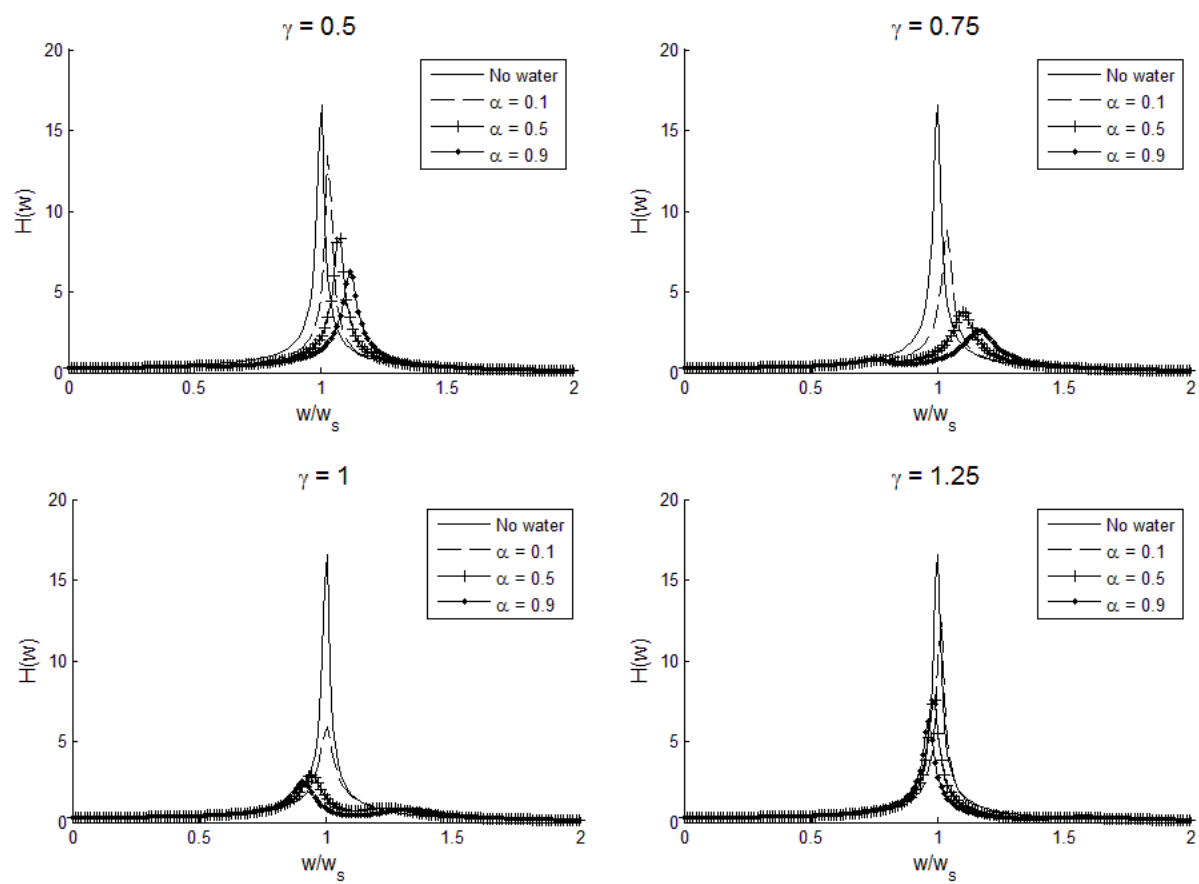


Figure 7

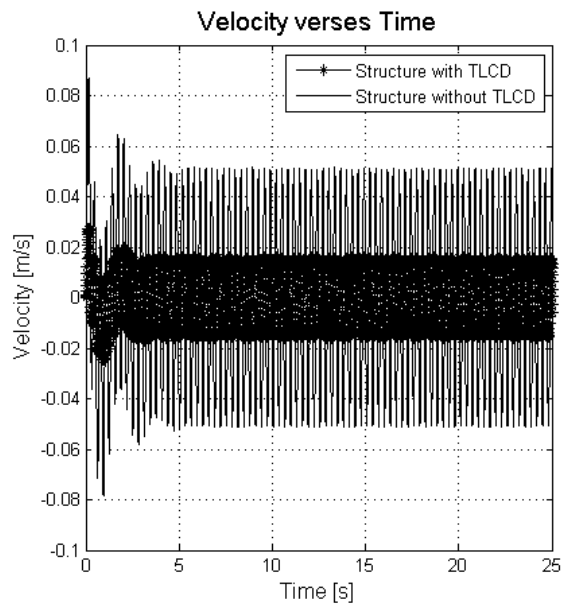
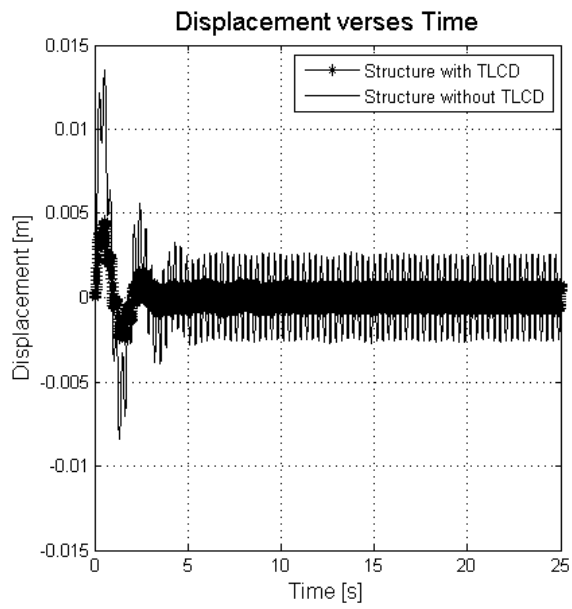


Figure 8

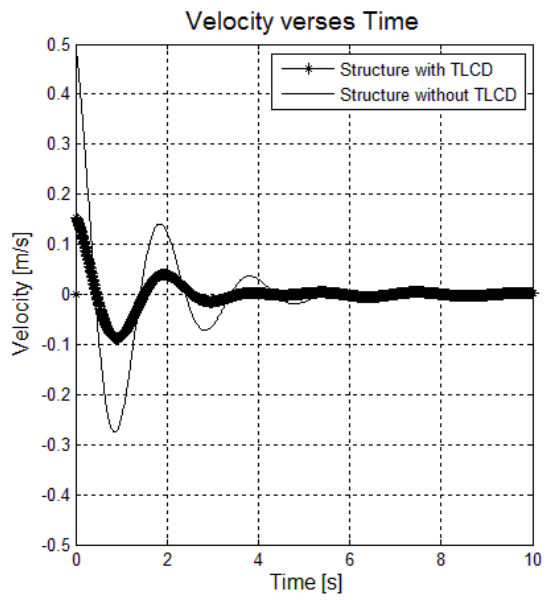
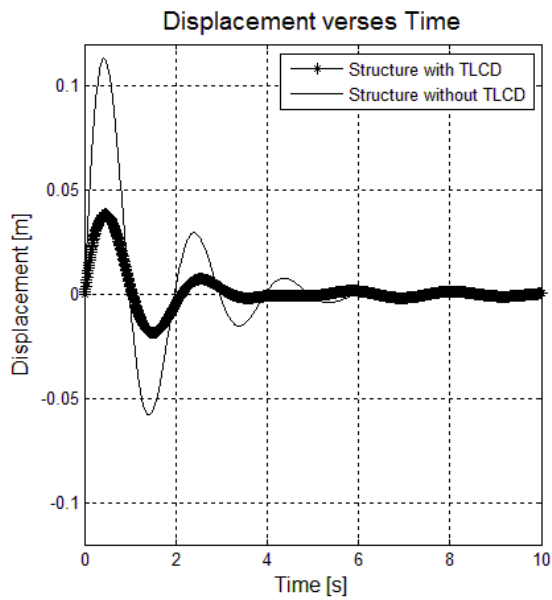


Figure 9

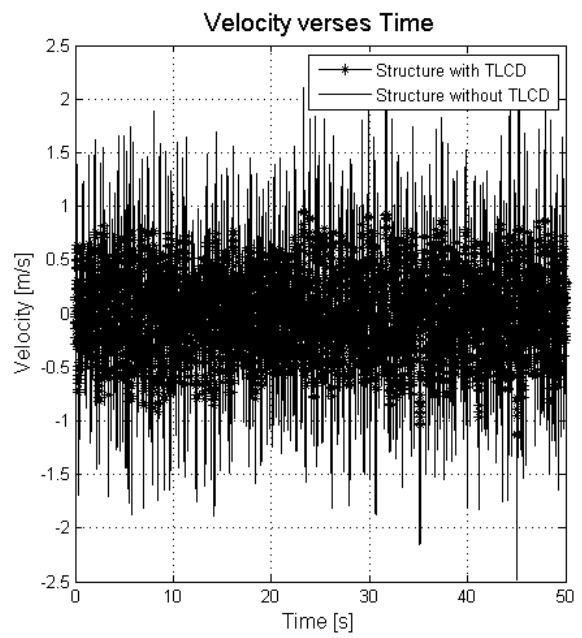
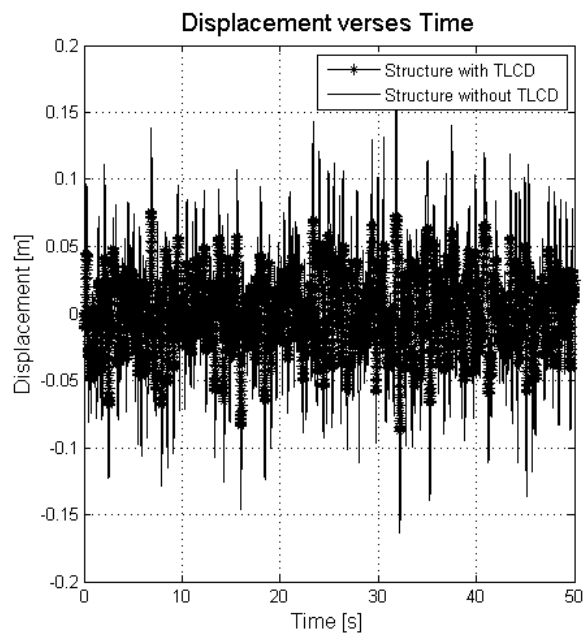


Figure 10

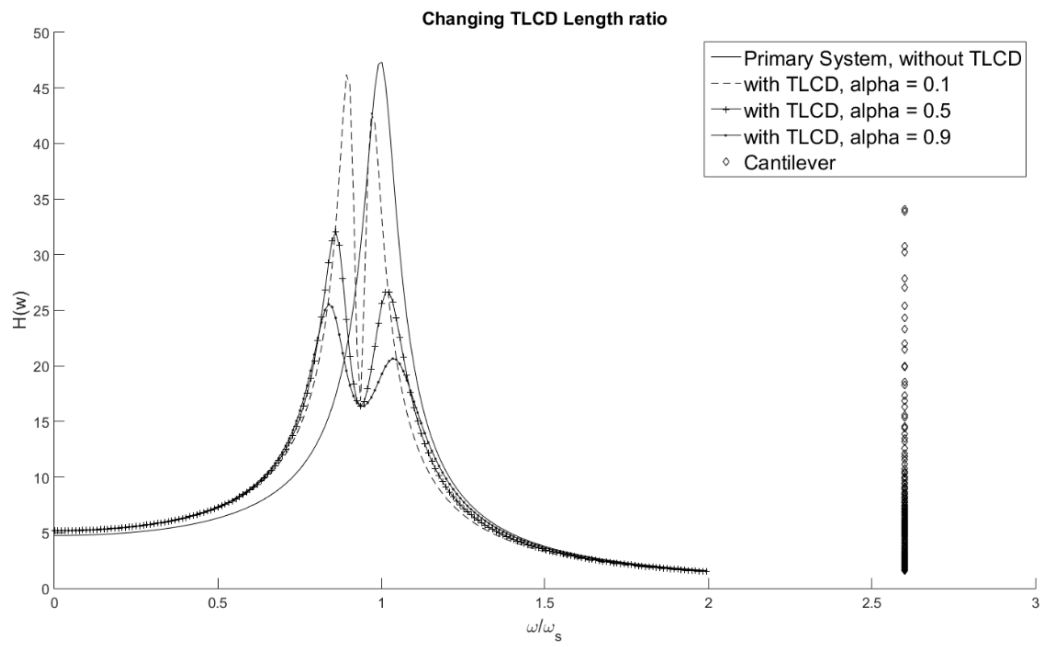


Figure 11

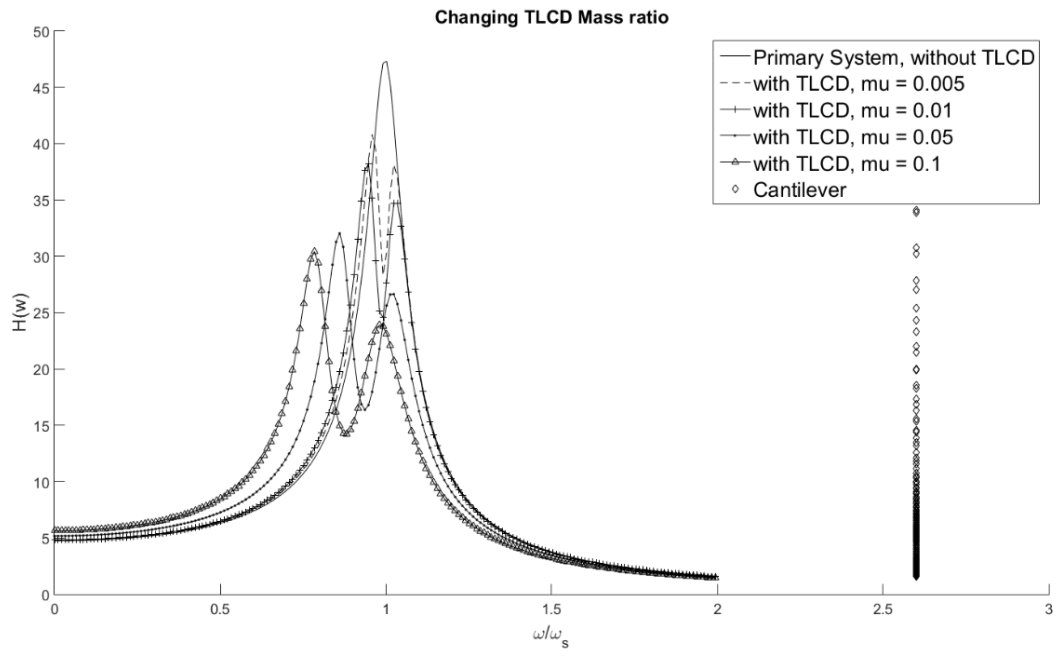
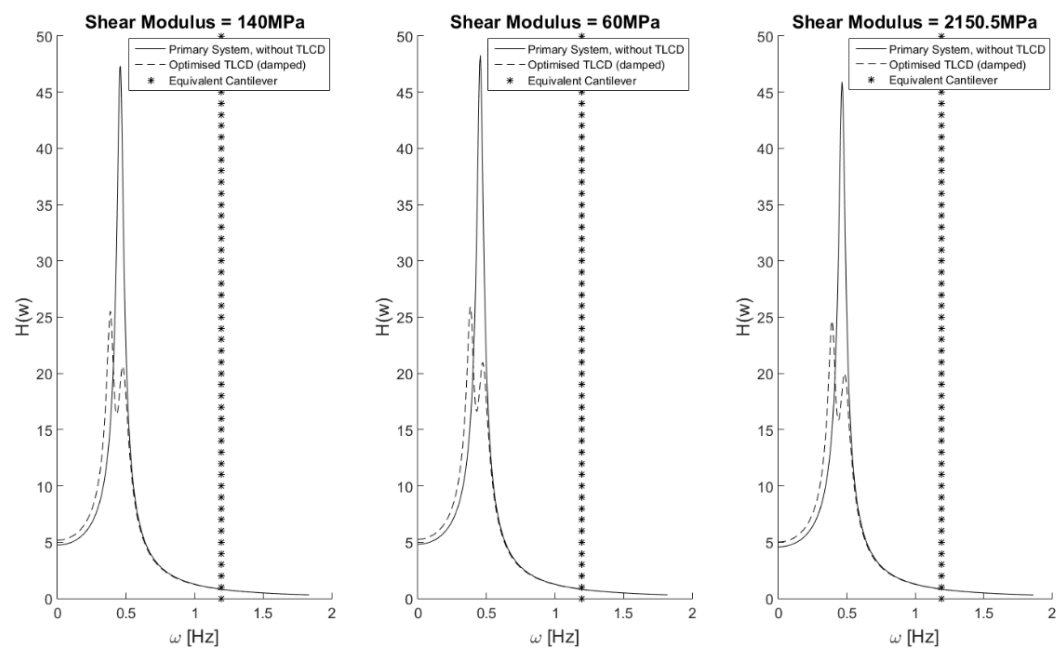


Figure 12

890



891

892

Figure 13

893

894

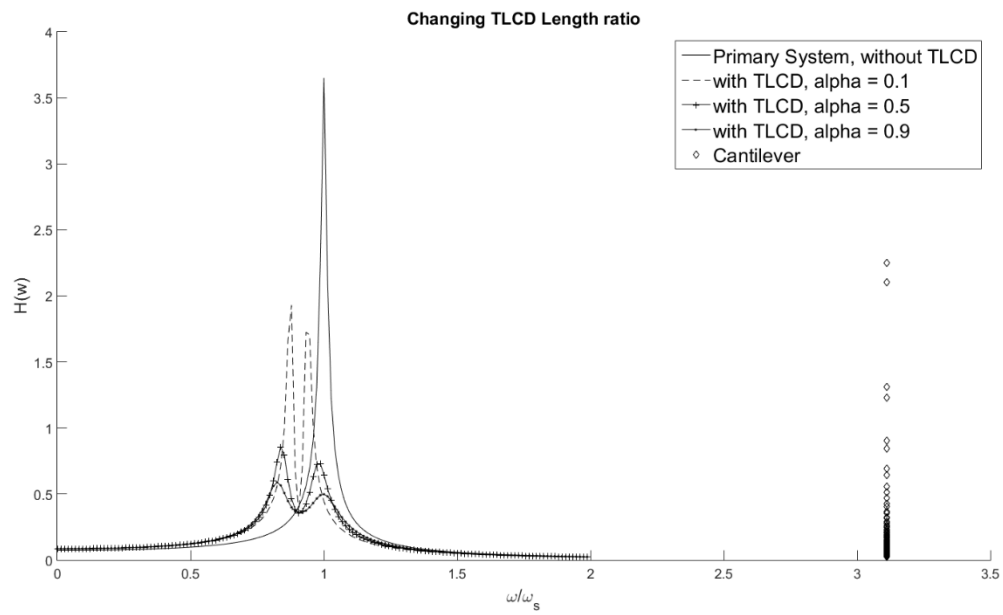
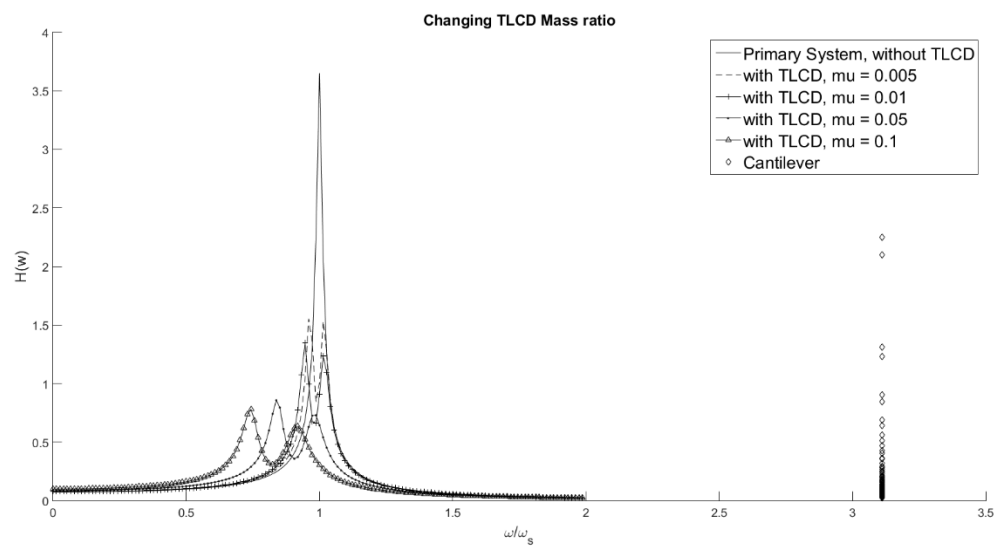


Figure 14

898



899

900

Figure 15

901

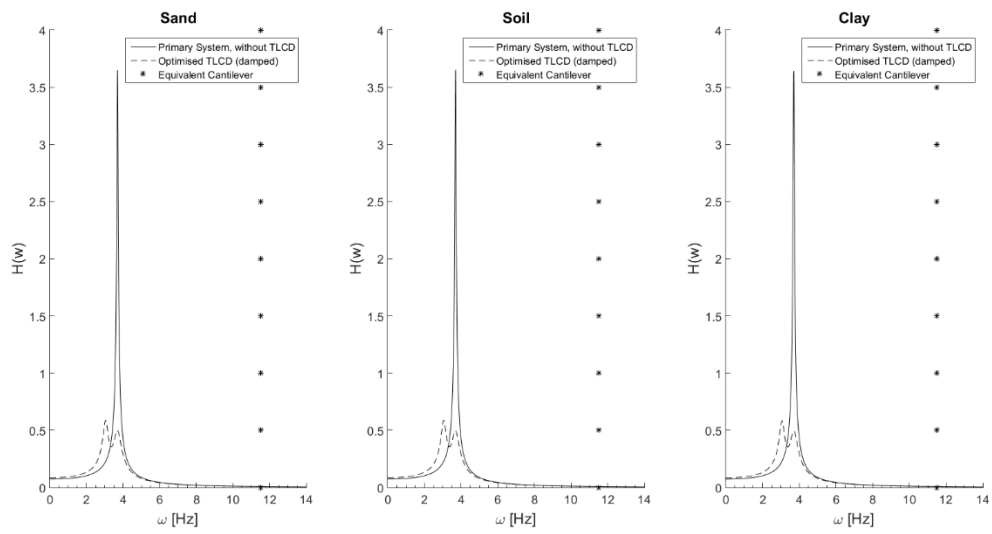


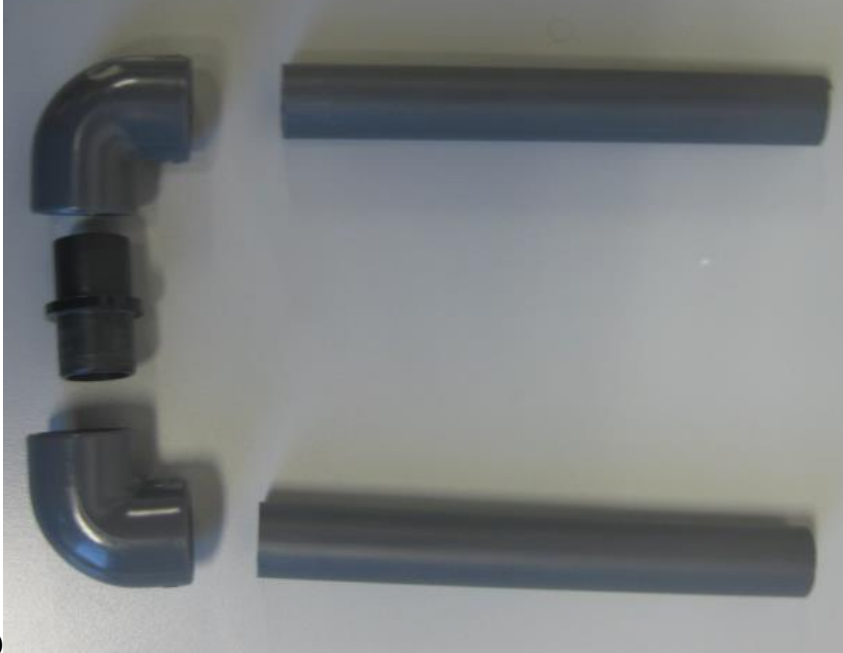
Figure 16

a)



b)





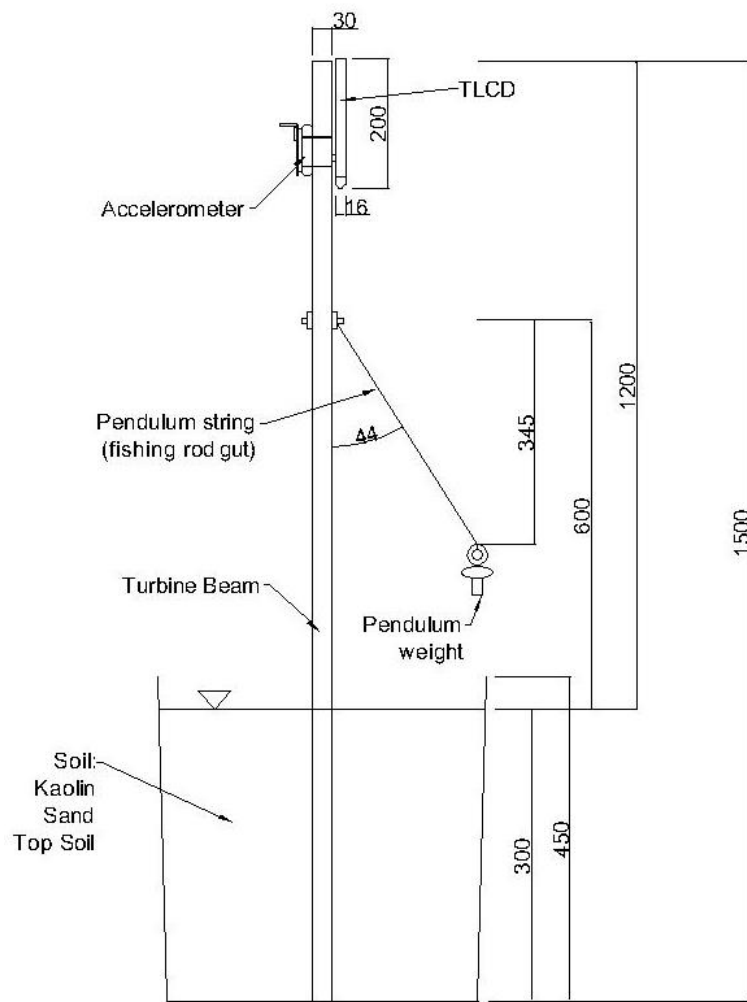
c)

914

Figure 17

915

TLCD-Offshore Wind Turbine, System



a)

b)

916

Figure 18

917

No water

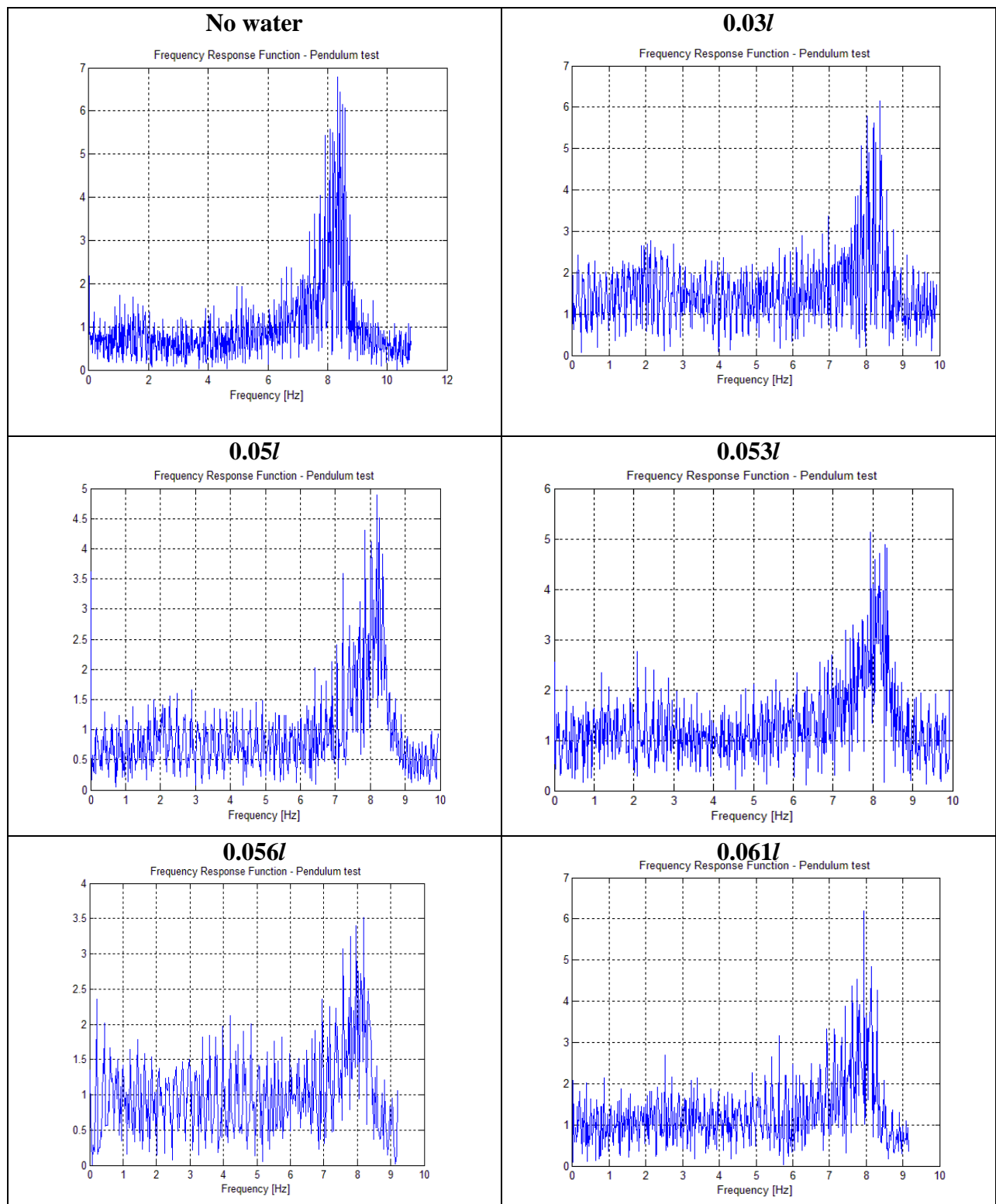
30ml

50ml

53ml

56ml

61ml



919

920

Figure 19

921

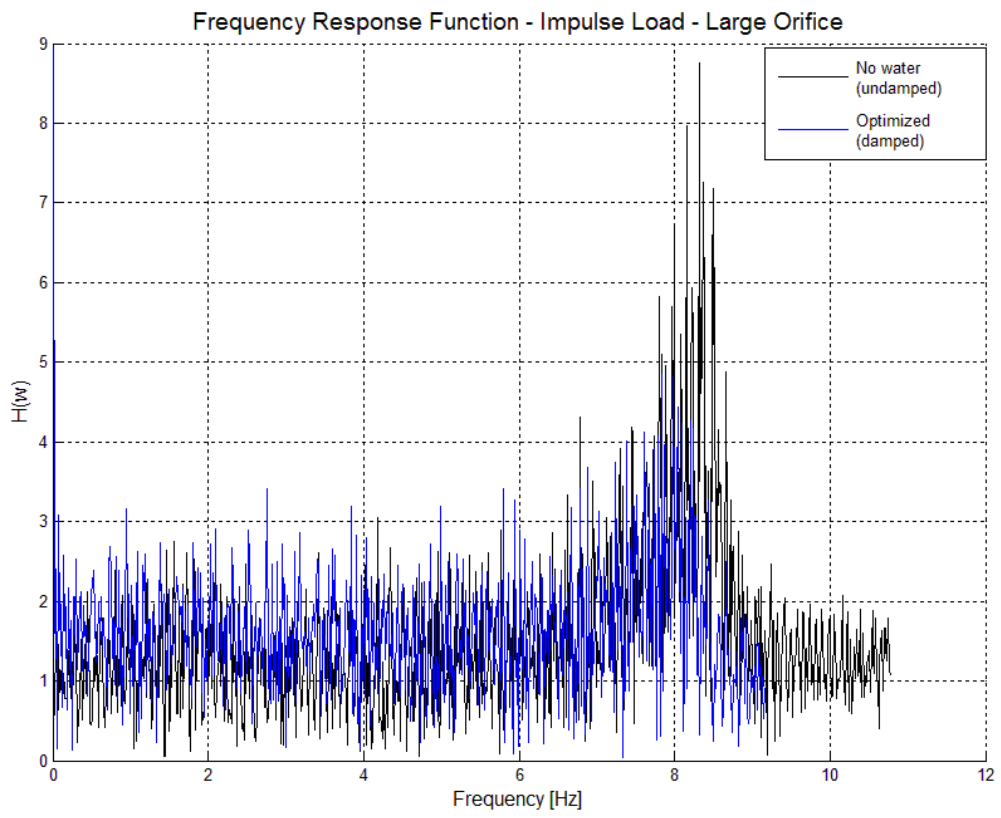


Figure 20